NPS-EC-99-006

NAVAL POSTGRADUATE SCHOOL
Monterey, California

Localization of Wireless Emitters Based on the Time Difference of Arrival (TDOA) and Wavelet Denoising

by

Ralph D. Hippenstiel
Tri T. Ha
Unal Aktas

May 1999

Approved for public release; distribution is unlimited.

Prepared for: TENCAP Office
Department of the Navy

NAVAL POSTGRADUATE SCHOOL
Monterey, California 93943-5000

RADM ROBERT C. CHAPLIN
Superintendent

R. Elster
Provost

This report was sponsored by the TENCAP Office, Department of the Navy.

Approved for public release; distribution unlimited.

The report was prepared by:

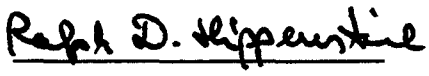

RALPH D. HIPPENSTIEL
Associate Professor
Department of Electrical and
Computer Engineering

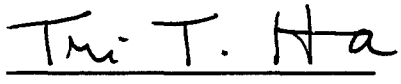

TRI T. HA
Professor
Department of Electrical and
Computer Engineering

Reviewed by:

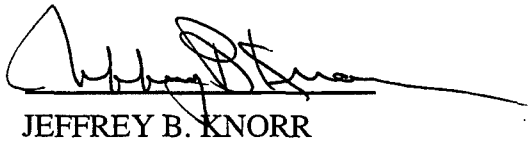

JEFFREY B. KNORR
Chairman
Department of Electrical and
Computer Engineering

Released by:

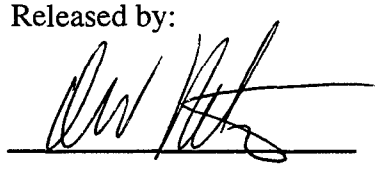

DAVID W. NETZER
Associate Provost and
Dean of Research

REPORT DOCUMENTATION PAGE

Form Approved
OMB No. 0704-0188

1. AGENCY USE ONLY (Leave blank)	2. REPORT DATE	3. REPORT TYPE AND DATES COVERED
	May 1999	Technical Report

4. TITLE AND SUBTITLE
Localization of Wireless Emitters Based on the Time Difference of Arrival (TDOA) and Wavelet Denoising

5. FUNDING NUMBERS
N4175698WR87397

6. AUTHOR(S)
Ralph D. Hippenstiel, Tri T. Ha, and Unal Aktas

7. PERFORMING ORGANIZATION NAME(S) AND ADDRESS(ES)
Department of Electrical and Computer Engineering
Naval Postgraduate School
Monterey, CA 93943-5000

8. PERFORMING ORGANIZATION REPORT NUMBER
NPS-EC-99-006

9. SPONSORING/MONITORING AGENCY NAME(S) AND ADDRESS(ES)
TENCAP Office
Department of the Navy, CNO/N632
2000 Navy Pentagon
Washington, D.C. 20350-2000

10. SPONSORING/MONITORING AGENCY REPORT NUMBER

11. SUPPLEMENTARY NOTES
The views expressed in this report are those of the author and do not reflect the official policy or position of the Department of Defense or the United States Government.

12a. DISTRIBUTION/AVAILABILITY STATEMENT
Approved for public release; distribution is unlimited.

12b. DISTRIBUTION CODE
A

13. ABSTRACT (Maximum 200 words)
The localization of mobile wireless communication units using time difference of arrival (TDOA) is studied. The wavelet transform is used to increase the accuracy of TDOA estimation. Several denoising techniques based on the wavelet transform are presented. These techniques are applied to different types of test signals and to a simulated baseband GSM signal. The results of the denoising techniques are compared to the ones employing no denoising in terms of the mean square error. The denoising techniques allow a 28 to 81 percent improvement in the TDOA estimation.

14. SUBJECT TERMS	15. NUMBER OF PAGES
time difference of arrival, wavelet, denoising, GSM	67
	16. PRICE CODE

17. SECURITY CLASSIFICATION OF REPORT	18. SECURITY CLASSIFICATION OF THIS PAGE	19. SECURITY CLASSIFICATION OF ABSTRACT	20. LIMITATION OF ABSTRACT
UNCLASSIFIED	UNCLASSIFIED	UNCLASSIFIED	SAR

Table of Content

I. INTRODUCTION

Reliable and accurate position information is important when locating mobile wireless communication units. One major commercial factor behind the recent interest in localization is the Federal Communications Commission (FCC) regulation [1] that requires wireless communications systems to provide Enhanced-911 (E-911) service. There are many other reasons where localization of wireless emitters is desirable or essential.

Our main focus is the reduction in mean square error for the time difference of arrival estimate, which in turn allows improved localization. Wavelet denoising, based on the modified approximate maximum likelihood (MAML), the fourth order moment, or their time varying adaptations, provides improvement.

A. POSITION LOCALIZATION SYSTEMS

A number of position localization systems have evolved over the years. Some of these position localization systems are *Global Positioning System (GPS)*, *Loran C*, and *Global Navigation Satellite System (GLONASS)*.

1. Global Positioning System (GPS)

GPS is the most popular radio navigation aid. GPS is also used to relay position of cellular phones to *public switched telephone networks* (PSTN) or to *public safety answering points* (PSAP). GPS obtains precise timing using a group of satellites that transmit a spread spectrum L-band signal centered at 1575.42 MHz [23]. Calculation of the distances to three different satellites, allows triangulation to determine the position of the cellular phone.

2. Loran C

Loran C is a navigational tool that operates in the low frequency (90-110 kHz) band and uses a pulsed hyperbolic system for triangulation. It has a repeatable accuracy in the 19-90 meters range and is accurate to about 100 meters with 95 percent confidence and 97 percent availability. Like GPS, its performance depends on local calibration and topography. GPS has replaced Loran C in most applications [13].

3. Global Navigation Satellite System (GLONASS)

The Global Navigation Satellite System (GLONASS) is similar system to GPS. GLONASS's synchronization time is 1/3 of GPS's, i.e., less than a minute [13].

B. METHODS FOR LOCATING CELLULAR PHONES

Localization techniques can be grouped into two categories. These are, position localization systems that require a modification of the existing handsets, and systems that require modification at the base stations. The second category consists of *angle of arrival* (AOA), *frequency difference of arrival* (FDOA), *time of arrival* (TOA), or *time difference of arrival* (TDOA) estimation of the wavefront at the receiving platforms.

1. Angle of Arrival (AOA)

A single platform may be sufficient for AOA localization of a wireless transmitter on the surface of the earth. Once the angle is determined, the position of the emitter can be obtained using the intersection of the centerline of the antenna beam, with the surface of the earth. The signals to the antenna must be coming from the *Line-Of-Sight* (LOS) direction. There is a considerable cost of installing antenna arrays and the method requires a relatively complex AOA algorithm [3, 13].

2. Frequency Difference of Arrival (FDOA)

FDOA measurements require at least two receiving platforms and a relative velocity, sufficiently large so that the differential Doppler shift of the two received signals is larger than the frequency measurement error.

3. Time of Arrival (TOA)

It may be possible for the base station to indirectly determine the time that the signal takes from the source to the receiver on the forward or the reverse link. The total time elapsed from the instant the command is transmitted to the instant the mobile response is detected, is composed of the sum of the round trip signal delay and any processing and response delay within the mobile unit. Due to the variations in design and manufacture of the handsets the time estimate is difficult to obtain. This method is susceptible to timing errors in the absence of LOS.

4. Time Difference of Arrival (TDOA)

The TDOA estimate is taken as the delay, which maximizes the cross-correlation function between signals arriving at two base stations. This also determines at which base station the signal arrives first. This information yields a hyperbolic localization curve. We can localize the wireless transmitter by solving two hyperbolic curve equations.

It is necessary that the code generators at each receiver be synchronized to have a common time base [2]. This form of localization is useful in asynchronous system since time of transmission need not be known. To determine the location of a transmitter in two dimensions, at least three receivers are required. If a major reflector effects the signal components going to all the receivers, the timing error may get reduced in the time difference operation.

II. GLOBAL SYSTEM FOR MOBILE (GSM)

GSM is a second-generation cellular system standard that was developed to solve the fragmentation problems of Europe's first cellular systems. GSM is the first cellular system to specify digital modulation, network level architectures and services. Prior to GSM it was not possible to use a given single subscriber unit throughout Europe. GSM was originally developed to serve as the Pan-European cellular service and promised a wide range of network service through the use of the *Integrated Services Digital Network (ISDN)*. GSM is now the world's most popular standard for cellular and personal communications equipment.

A. GSM SYSTEM ARCHITECTURE

The GSM system architecture consists of three major interconnected subsystems that interact with themselves and the users through network interfaces. The subsystems are the *Base Station Subsystem* (BSS), *Network and Switching Subsystem* (NSS), and the *Operation Support Subsystem* (OSS). *The Mobile Station* (MS) is also a subsystem, but is usually considered to be part of the BSS for architectural purposes.

The BSS provides and manages radio transmission between the MS's and the Mobile Switching Center (MSC). The BSS also manages the radio interface between the MS's and all other subsystems of GSM.

The NSS manages the switching functions of the system and allows the MSC's to communicate with other networks such as the *Public Switched Telephone Network* (PSTN) and *Integrated Services Digital Network* (ISDN).

The OSS supports the operation and the maintenance of GSM and allows system engineers to monitor, diagnose, and troubleshoot all aspects of GSM. This subsystem interacts with the other GSM subsystems.

1. GSM Signal Specifications

GSM utilizes two 25 MHz bands, which have been set aside for system use in all member countries. The 890-915 MHz band is used for subscriber-to-base transmission (reverse link), and the 935-960 MHz band is used for base-to-subscriber transmission (forward link). GSM uses *Frequency Division Duplex* (FDD) and a combination of *Time Division Multiple Access* (TDMA) and *Frequency Hopped Multiple Access* (FHMA) schemes to provide stations with simultaneous access to multiple users. The available forward and reverse frequency bands are divided into 200 KHz channels. These channels are identified by their *Absolute Radio Frequency Channel Number* (ARFCN). The ARFCN denotes a forward and reverse channel pair, which is separated in frequency by 45 MHz. Each channel is time shared between as many as eight subscribers using TDMA.

The radio transmissions on both forward and reverse link are made at a channel data rate of 270.833 Kbps using binary *0.3 GMSK* modulation. The bandwidth-bit duration product, *BT,* has a level of 0.3. The signaling bit duration is 3.692 μs. User data is sent a maximum rate of 24.7 Kbps. Each time slot (TS) has an equivalent time allocation allowing for 156.25 channel bits. From this, 8.25 bits of guard time and 6 total start and stop bits are used to prevent overlap with adjacent time slots. Each TS has a time duration of 576.92 μs, while a single GSM TDMA frame spans 4.615 ms. The total

number of available channels within a 25 MHz bandwidth is 125. Table 2.1 summarizes the signal specifications [5].

Parameter	**Specifications**
Reverse Channel Frequency	890-915 MHz
Forward Channel Frequency	935-960 MHz
ARFCN Number	0 to 124 and 975 to 1023
Tx/Rx Frequency Spacing Tx/Rx Time Slot Spacing	45 MHz 3 Time slots
Modulation Data Rate	270.833333 Kbps
Frame Period	4.615 ms
Users per Frame (Full Rate)	8
Time Slot Period	576.9 μs
Bit Period	3.692 μs
Modulation	0.3 GMSK
ARFCN Channel Spacing	200 KHz
Interleaving (max delay)	40 ms
Voice Coder Bit Rate	13.4 Kbps.

Table 2.1: GSM signal specifications.

2. Gaussian Minimum Shift Keying (GMSK)

GMSK is a binary modulation scheme which may be viewed as a derivative of *Minimum Shift Keying* (MSK). In GMSK, the sidelobe levels of the spectrum are reduced by passing the modulating *Non-return to zero* (NRZ) data waveforms through a pre-modulation Gaussian pulse-shaping filter [12]. Baseband Gaussian pulse shaping smoothes the phase trajectory of the MSK signal and hence stabilizes the instantaneous frequency variations over time. This reduces the sidelobe levels of the transmitted spectrum.

3. GSM Channel Types

There are two types of GSM logical channels, called *traffic channels* (TCH) and *control channels* (CCH). Traffic channels carry digitally encoded user speech or data and

have identical functions and formats on the forward and reverse link. Control channels carry signaling and synchronizing commands between the base and mobile station.

4. Frame Structure for GSM

There are eight time slots (TS) per GSM frame. The frame period is 4.615 ms. A TS consists of 148 bits which are transmitted at rate of 270.833 Kbps (an unused guard time of 8.25 bit period is provided at the end of each burst). Out of the total 148 bits per TS, 114 are information bits, which are transmitted as two 57 bit sequences close to the beginning and end of the burst. A 26 bit training sequence allows the adaptive equalizer in the mobile or base station receiver to analyze the radio channel characteristics before

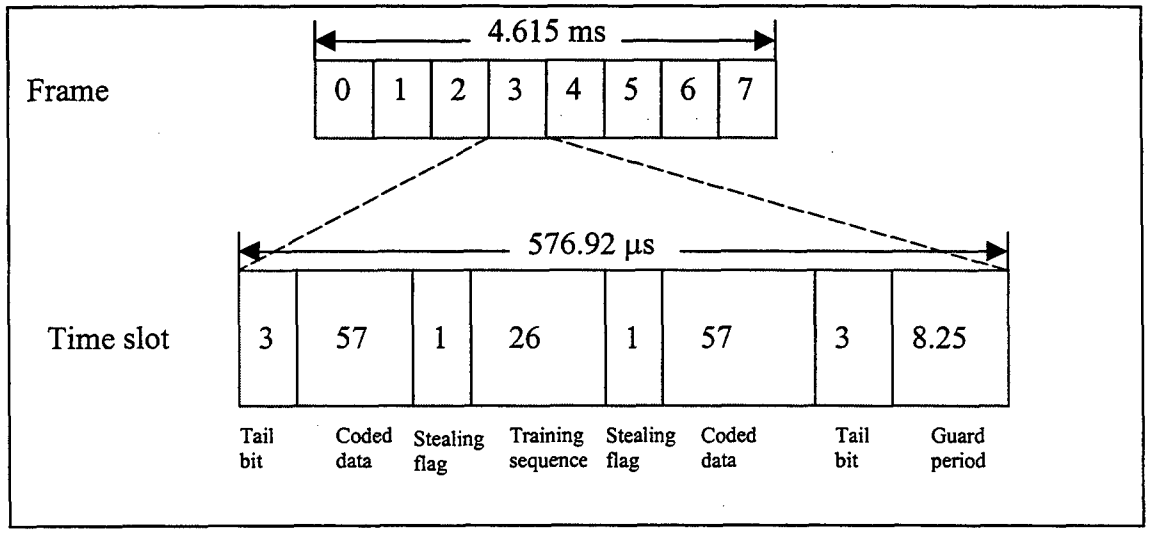

Figure 2.1: GSM frame structure.

decoding the user data. Stealing flags on the both side of the training sequence are used to distinguish whether the TS contains voice or control data.

B. TRANSMITTER/RECEIVER SYSTEM

In this section we will look at the GSM transmitter and receiver and simulate some GSM

signals to be used for simulation purposes. The overall structure of the GSM transmitter/receiver system is illustrated in Figure 2.2.

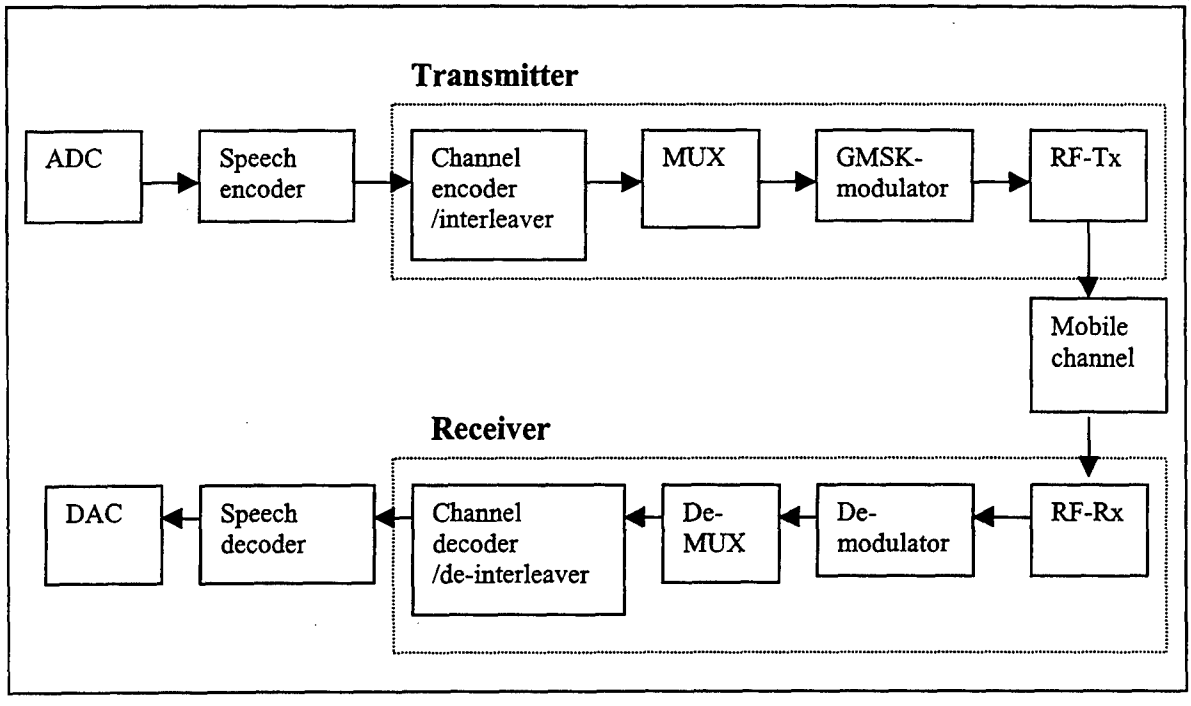

Figure 2.2:Block diagram for the GSM transmitter/receiver system.

1. Transmitter Structure

The overall structure of the transmitter is illustrated in Figure 2.3. The transmitter consists of four distinct functional blocks.

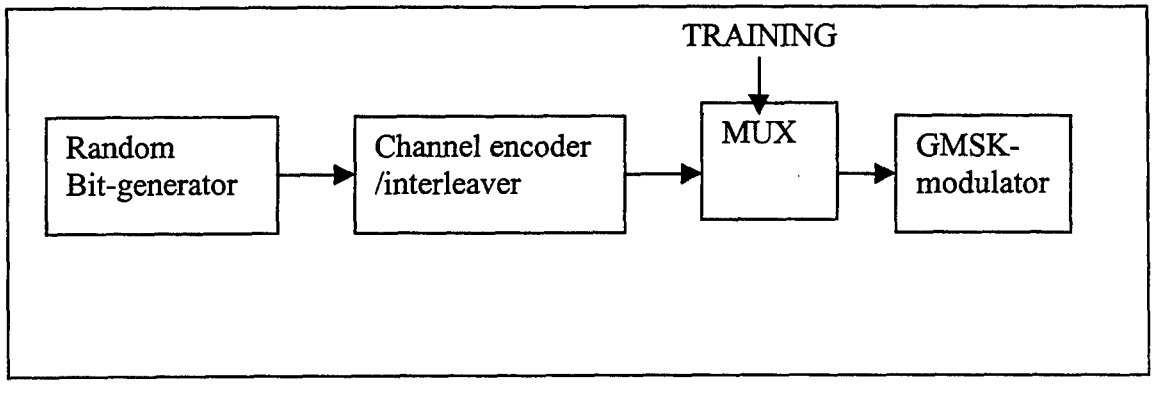

Figure 2.3: The overall structure of the transmitter.

To simulate an input data stream to the channel encoder/interleaver, a sequence of random data bits is generated. This sequence is accepted by the MUX, which splits the incoming sequence to form a GSM normal burst. The burst type requires that a training sequence is supplied and included. Upon having generated the prescribed GSM normal burst data structure, the MUX sends this to the GMSK-modulator. The GMSK-modulator block performs a differential encoding of the incoming burst to form a NRZ sequence. This modified sequence is then subject to the actual GMSK-modulation after which, the resulting signal is represented as a complex I and Q baseband signal.

2. Receiver Structure

The general structure of the receiver is illustrated in Figure 2.4. The demodulator accepts the GSM burst, r, using a complex baseband representation. Based on this data sequence, knowing the oversampling rate *OSR*, the training sequence *TRAINING* , and the desired length of the receiving filter, *Lh*, the demodulator determines a bit sequence. This demodulated sequence is then used as the input to the demultiplexer (DeMUX) where the actual data bits are obtained. The remaining control bits and the training sequence are stripped off. Finally channel decoding and de-interleaving is performed.

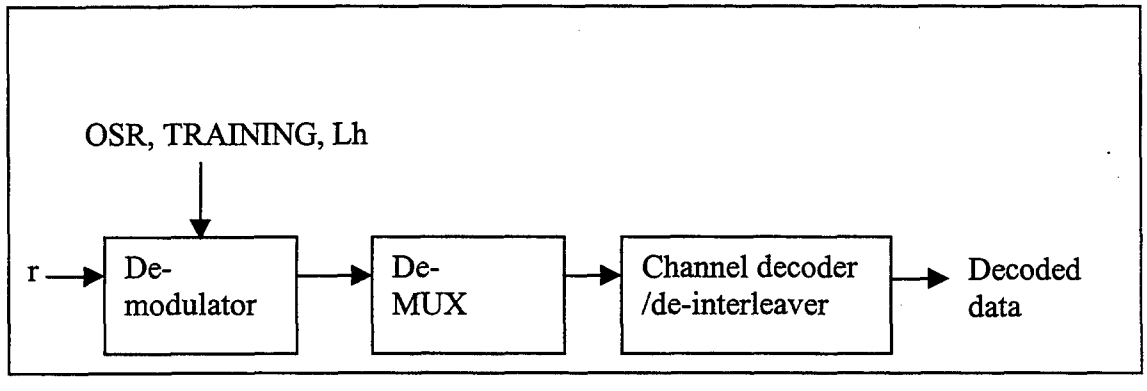

Figure 2.4: The overall structure of the receiver.

III. WAVELETS

Transforms are used to obtain information that is not observable in the original signal. The wavelet transform provides a time-scale representation [6]. There are other transformation, which can give similar information, such as the short time Fourier transform, the Wigner-Ville distribution, etc. This chapter will initially discuss Fourier and then present wavelet analysis.

A. FOURIER ANALYSIS

Fourier analysis breaks a signal into its constituent sinusoidal components. One can think of the Fourier analysis as a mathematical technique for transforming the signal from a time-based to a frequency-based representation [7].

1. Fourier Series

Let $g_p(t)$ denote a periodic signal with period T_0. By using the Fourier series expansion, we can express the signal as a weighted sum of complex exponentials [8]:

$$g_p(t) = \sum_{n=-\infty}^{\infty} c_n e^{j2\pi n f_0 t} \quad , \qquad (3.1)$$

where $f_0 = 1/T_0$ and c_n is given by

$$c_n = \frac{1}{T_0} \int_{-T_0/2}^{T_0/2} g_p(t) e^{-j2\pi n f_0 t} dt \quad , \quad n = 0, \pm 1, \pm 2, \cdots \quad . \qquad (3.2)$$

2. Fourier Transform

The Fourier transform of a general continuous function *g(t)* is defined as [8]:

$$G(f) = \int_{-\infty}^{\infty} g(t) e^{-j2\pi f t} dt \quad . \qquad (3.3)$$

$G(f)$ is a continuous function of the variable f. The signal $g(t)$ can be recovered by [8]:

$$g(t) = \int_{-\infty}^{\infty} G(f)e^{j2\pi ft}df \,. \qquad (3.4)$$

The functions $g(t)$ and $G(f)$ are known as a *Fourier transform pair.*

Fourier analysis is extremely useful because the signal's frequency content is of great importance, but in transforming to the frequency domain, time information is lost. However, many signals contain non-stationary or transitory characteristics such as trends, or abrupt changes. These characteristics can be the most important part of the signal.

3. Short-Time Fourier Analysis

The short-time Fourier transforms (STFT) is an extension of the Fourier transform designed to map the signal into the time-frequency plane. The STFT uses a sliding window function $w(t)$ to segment the data. The STFT is given by

$$S(\tau, f) = \int_{-\infty}^{\infty} g(t)w^*(t-\tau)e^{-j2\pi ft}dt \,, \qquad (3.5)$$

where $w^*(t-\tau)$ is the sliding window, * represents conjugation. The window function, $w(t)$, affects the characteristics of STFT. As a result of the uncertainty principle, the time resolution (Δt), and the frequency resolution (Δf) of a given signal are inversely related. Their product has lower bound of $1/4\pi$, which is achieved by the Gaussian window [9]. This produces a trade-off in resolution of time and frequency. Since the choice of window will fix (Δt) and (Δf) for the entire time axis, the STFT partitions the time-frequency plane into a uniform grid. The window can not provide good time resolution and good frequency resolution simultaneously [22].

B. WAVELET ANALYSIS

1. Introduction

A wavelet is an oscillatory function [10]. It has its energy concentrated in time, which allows the analysis of transient, non-stationary, or time-varying phenomena.

2. The Continuous Time Wavelet Transform (CTWT)

The continuous time wavelet transform (CTWT) is defined as :

$$C(\tau,a)=\frac{1}{\sqrt{a}}\int_{-\infty}^{\infty}g(t)\,\Psi^{*}\left(\frac{t-\tau}{a}\right)dt, \qquad (3.6)$$

where $\Psi(t)$ is the wavelet function, τ is the translation in time, a denotes dilation or compression in time, $1/\sqrt{a}$ normalizes the energy and * denotes conjugation.

The time and frequency resolution is controlled by the scale factor a. Low scales correspond to high frequency wavelets and provide good time resolution. High scales correspond to low frequency wavelets with poor time but good frequency resolution. The time-frequency mapping of the STFT and CWT is shown in Figure 3.1.

The STFT produces a uniform grid with a constant time (Δt) and frequency resolution (Δf), while the CTWT has a time and frequency resolution that depends on the scale.

3. The Discrete Wavelet Transform (DWT)

Although the discretized continuous wavelet transform enables the computation of the continuous wavelet transform by computers, it is not a true discrete transform [6]. As a matter of fact, the wavelet coefficients are simply a sampled version of the CWT, and the information it provides is highly redundant, as far as the reconstruction of the signal is concerned. This redundancy, on the other hand, requires a significant amount of computation time and resources.

The DWT provides sufficient information, and can offer a significant reduction in

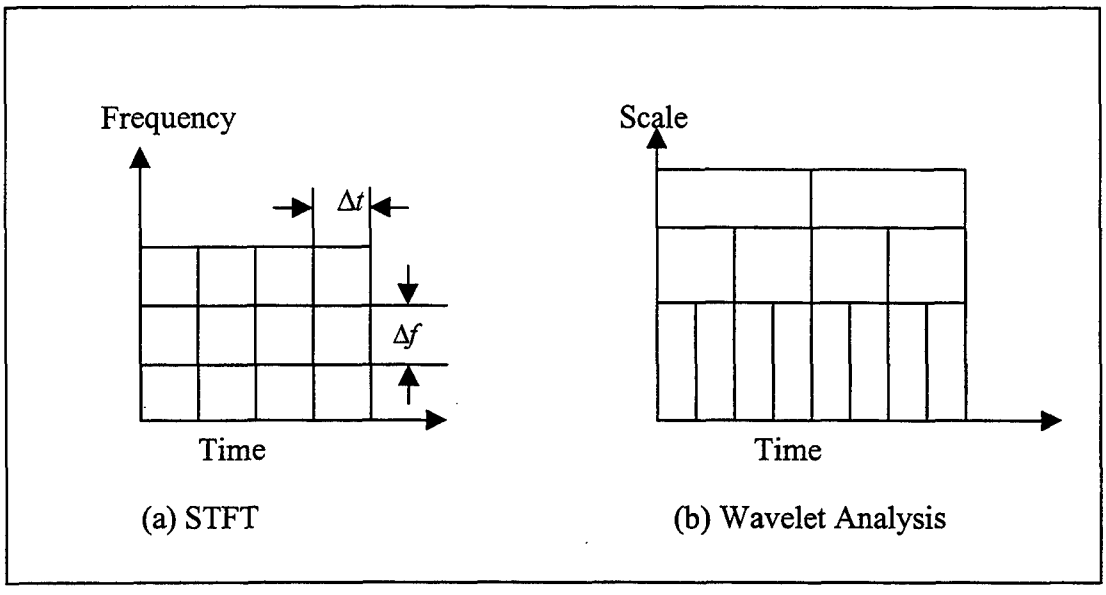

Figure 3.1: (a) Frequency-Time plane for STFT, (b) Scale-Time plane for CWT.

the computation time. It is considerably easier to implement than the continuous wavelet transform and obtained by restricting the scale and time parameters of the CWT to discrete values. The DWT of a discrete signal g(n) is defined by

$$C(a,b) = \sum_n \frac{1}{\sqrt{a}} g(n) \Psi^* \left(\frac{n-b}{a} \right), \qquad (3.7)$$

where a, b, and n are the discrete versions of a, τ, and t of Equation 3.6 respectively. The scaling factor is further restricted to;

$$a = a_0^J, \qquad \text{J=0,1,...} \log_2(N). \qquad (3.8)$$

The choice of a_0 will govern the accuracy of the signal reconstruction via the inverse transform. It is popular to choose a_0=2, since it permits the implementation of fast algorithms. Setting $a = 2^J$ produces octave bands called dyadic scales. As the scale level is increased from J to J+1, the analysis wavelet is stretched in the time domain by a factor

of two. Hence the DWT output has better frequency resolution and less precise time resolution as the scale number increases.

If the time shifting parameter b is restricted to $k2^J$, where k is an integer, this version of the DWT is known as the decimated DWT and can be written as:

$$C(2^J, k2^J) = \sum_{n=1}^{N} \frac{1}{\sqrt{a}} g(n)\Psi^*\left(2^{-J}n - k\right); \qquad (3.9)$$

where $J = 0, 1, 2, \cdots, \log_2(N)$, $k = 1, 2, \cdots, N2^{-J}$, and N is the length of the signal *g(n)*. The term $k2^J$ in the argument of DWT, indicates that *C(a, b)* is decimated by a factor of two at each successive scale J retaining only the even points.

a. Subband Coding and Multiresolution Analysis

The time-scale (frequency) representation of the signal is obtained by using digital filtering techniques. Filters of different cutoff frequencies are used to analyze the signal at different scales. The signal is passed through a series of high pass filters and low pass filters. Each one of the filter is followed by a two-to-one decimator.

The DWT analyzes the signal at different frequency bands with different resolutions by decomposing the signal into a coarse and a detail component at each scale. The DWT employs two sets of functions, a scaling (low pass) and a wavelet (high pass) function. The decomposition of the signal into different frequency bands is obtained by successive highpass and lowpass filtering of the signal followed by the decimation operation.

This decomposition halves the time resolution, since the output is characterized by half the number of samples compared to the input signal. This operation

doubles the frequency resolution, since the frequency band of the signal now spans only half the input frequency band. This procedure, known as subband coding, is repeated.

b. WAVELET ANALYSIS

Wavelet transforms are very efficient and effective in analyzing a wide class of signals [10].

1. The wavelet transform allows a more accurate time description and identification of signal characteristics. A wavelet coefficient represents a component that is localized in time. The wavelet transform may allow a separation of components of a signal that overlap in time or frequency.

2. Wavelets are adaptable and can be designed to fit individual applications. The discrete wavelet transform is well suited to digital implementation.

IV. TIME DIFFERENCE OF ARRIVAL (TDOA) ESTIMATION

TDOA can be employed to find the position of a GSM emitter. Figure 4.1 shows a typical configuration; one emitter and a pair of receivers (discrete time).

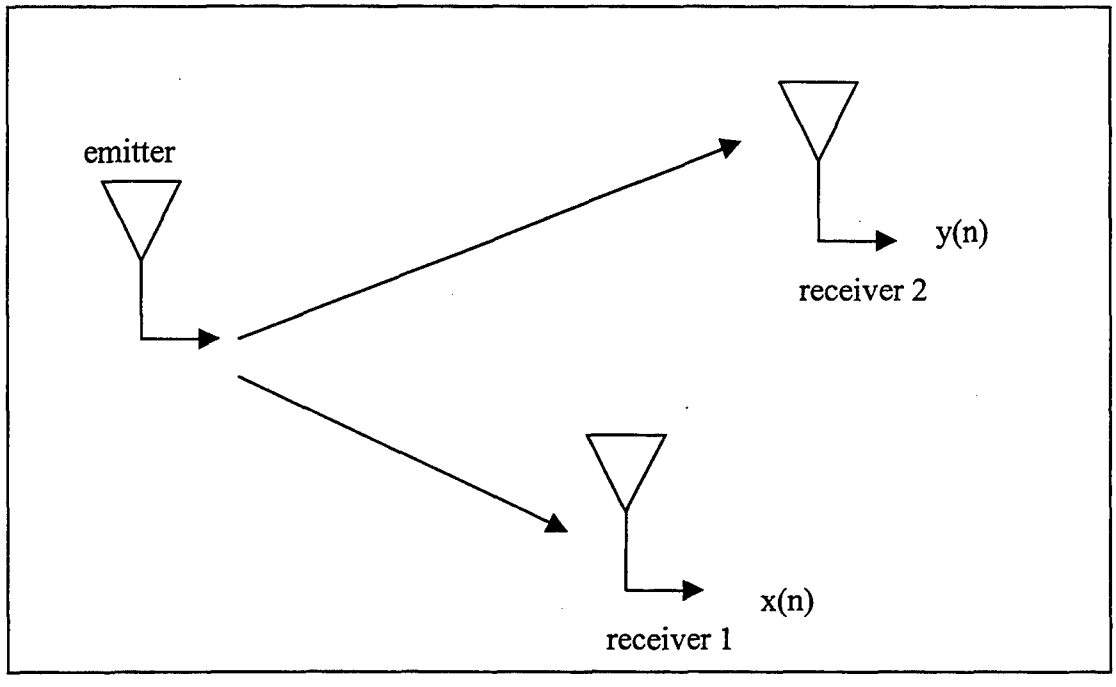

Figure 4.1: One transmitter-two receiver configuration.

A. CORRELATION FUNCTION

Frequently we would like to know the association between two signals, that is, how one signal is related to the other. Correlation of signals is often encountered in radar and sonar processing, and digital communications.

Suppose that the signal at receiver one is denoted by *x(n),* while *y(n)* is a time shifted version of *x(n)* at receiver 2. With additive noise, *x(n)* and *y(n)* can be modeled as:

$$x(n) = s(n) + n_1(n) \qquad (4.1)$$

$$y(n) = \alpha s(n-D) + n_2(n) \qquad , n = 0, 1, \cdots, N-1 \qquad (4.2)$$

where *s(n)* is the unknown source signal, $n_1(n)$ and $n_2(n)$ are additive noise, D is the difference in arrival times at the receivers, α is an attenuation coefficient, and N is the number of samples in each snap shot received at the two receivers.

The most widely accepted method for obtaining TDOA (D in Equation 4.2) uses the cross correlation method. Expectation of x(n) and y(n) leads to

$$\begin{aligned} R_{xy}(\tau) &= E\{x(n)y(n-\tau)\} \\ &= E\{\alpha s(n)s(n-D-\tau) + s(n)n_2(n-\tau) + \alpha s(n-D-\tau)n_1(n) + n_1(n)n_2(n-\tau)\}. \end{aligned}$$

Since the noise and signal are independent, and the noise has zero mean, the cross terms of the expectation are zero. Also the noise is independently distributed, so the expectation of $n_1(n)$ and $n_2(n-\tau)$ is also zero. The cross correlation of x(k) and y(k) becomes

$$R_{xy}(\tau) = \alpha R_s(D+\tau) \quad . \qquad (4.3)$$

Figure 4.2 shows the circuit and the block diagram for the discrete time cross correlator. The cross correlation approach requires that receivers share a precise time reference. The performance of the TDOA estimates can be improved by increasing the summation interval. Once the cross correlation function is computed, the value of τ which maximizes Equation 4.3 is used as the estimate of the TDOA. Figure 4.3 displays the fast correlation method. A cross spectral density estimate is obtained in the frequency domain, and the cross correlation estimate is obtained via an inverse Fourier transform.

B. SIMULATION

Two hundred simulations are used to evaluate the performance of the TDOA method.

The i^{th} error is given by $\quad e_i = D - \hat{D}_i \quad i = 1, 2, \cdots, N \ , \qquad (4.4)$

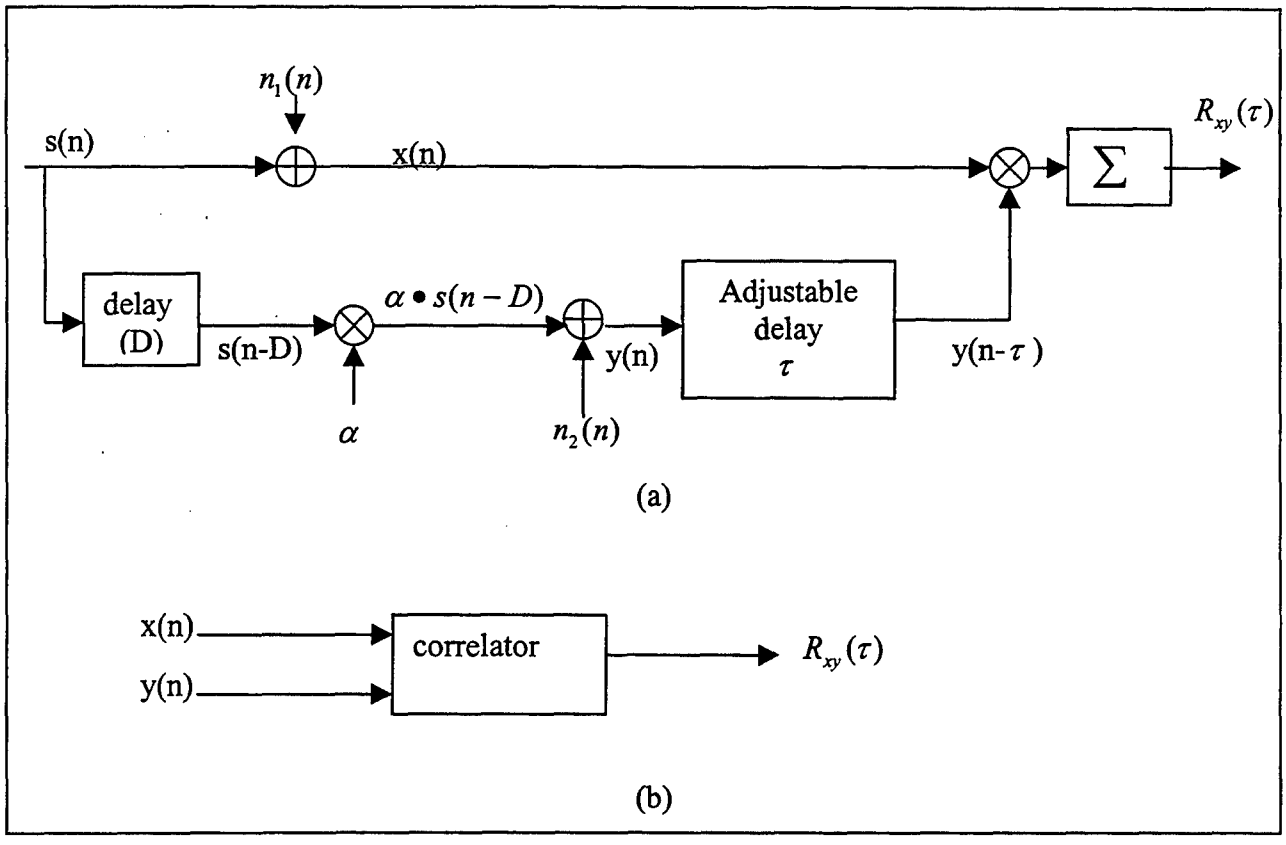

Figure 4.2: (a) Detail of the cross correlator (b) Block diagram for the cross correlator.

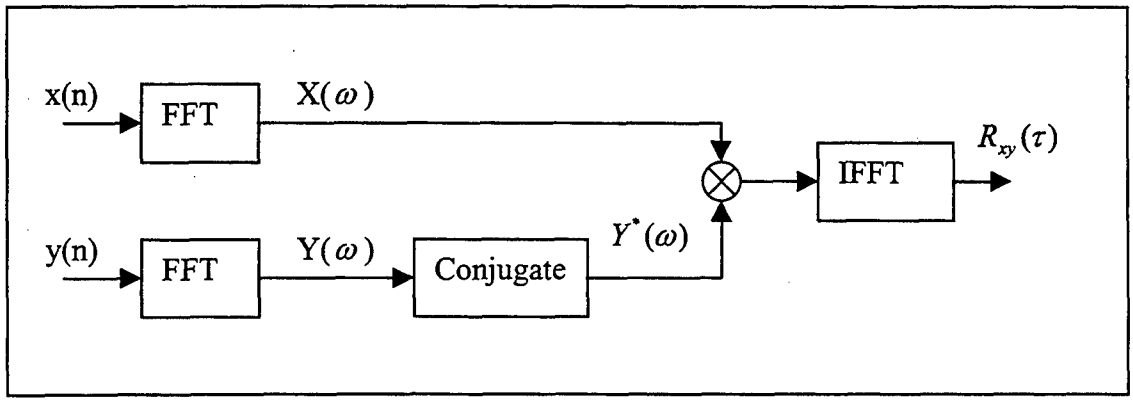

Figure 4.3: Fast cross correlation method using fast Fourier transforms.

where N is the number of realizations. The mean square error (MSE) is given by

$$MSE = \frac{1}{N}\sum_{i=1}^{N}|e_i|^2 \quad , \qquad (4.5)$$

where e_i is the error for the i^{th} realization.

V. WAVELET DENOISING

One important wavelet transform applications is noise reduction. The basic idea of denoising is to retain the coefficients that preserve the signal while removing those that represent noise. Two main properties of the wavelet transform assist in separating the noise coefficients from the rest. The first one is that, by choosing the basis function to match the signal, the resulting decompositions will contain relatively few coefficients. The second one is that, for a Gaussian noise input, the transform coefficients will remain Gaussian [18].

Wavelet shrinkage, introduced by Donoho and Johnstone [18-20], retains the coefficients above a given level. It discards the ones below the given level. Denoising consists of three steps.

1. Taking the wavelet transform of the input signal.
2. Selecting a threshold and suppressing the noisy coefficients by applying a non-linear thresholding technique.
3. Performing the inverse wavelet transform using the modified coefficients.

A. THRESHOLD VALUES

The term threshold refers to a constant that is computed. It separates the coefficients that are to be retained from those that are not. The noisy data can be written as,

$$x(n)=s(n)+\sigma n(n) \qquad n=0,1,2,\cdots,N\ , \qquad (5.1)$$

where $s(n)$ is the input signal to be recovered from the noisy data, $n(n)$ is zero mean, unit variance additive white Gaussian noise (AWGN), N is the length of the signal, σ is the

standard deviation of the AWGN. Algorithms computing the threshold value T require estimation of σ. Five methods of computing thresholds are described below.

1. Stein's Unbiased Risk Estimator (SURE) Threshold (T_{SU})

This method of threshold calculation was proposed by Donoho and Johnstone [20]. The thresholding is adaptive: A threshold level is assigned to each dyadic resolution level by the principle of minimizing the Stein Unbiased Estimate of Risk (SURE) [21] for threshold estimates. The SURE threshold is smoothness adaptive. If the unknown signal contains jumps, the reconstruction does also. If the unknown signal has a smooth segment, the reconstruction is as smooth as the mother wavelet will allow. This statistical procedure calculates the estimated mean square error (risk) for a range of threshold values, and selects T_{SU} with the resulting minimum risk.

2. Sqtwolog Threshold (T_{sq})

Sqtwolog threshold uses a fixed form threshold yielding minimax performance multiplied by a small factor proportional to *log(length(signal))* [7]

$$T_{sq} = \sqrt{2\log(length(signal))} \quad . \qquad (5.2)$$

3. Heursure Threshold (T_h)

Heursure threshold is mixture of SURE and sqtwolog threshold methods [7].

4. Minimaxi Threshold (T_m)

Minimaxi threshold uses a fixed threshold chosen to yield mimimax performance for mean square error against an ideal procedure [7]. The minimax principle is used in statistics in order to design estimators. It is designed to select estimators that minimize the worst case error occurring in the set.

5. Wo-So-Ching Threshold (T_{wsc})

This threshold method was proposed by Wo, So, and Ching. It will be discussed in detail in Chapter VI.

The threshold techniques, 1 through 4, are part of Donoho's method. Details are discussed in Chapters VI and VII. At the low SNR levels Donoho's method did not provide an improvement. Threshold technique 5 was used successfully and details are discussed in Chapter VI and VII.

B. THRESHOLDING (SHRINKAGE)

Once a threshold value is established, a number of methods exist to apply the threshold to suppress or modify the coefficients of the decomposition. We examined three thresholding methods.

1. Hyperbolic Thresholding

Hyperbolic thresholding was proposed by Wong and will be discussed in detail in Chapter VI.

2. Hard Thresholding

Hard thresholding can be described as the usual process of setting to zero the elements whose absolute values are lower than the threshold [7]. For notational convenience, we define *x(n)* and *n(n)* as vectors.

$$\begin{aligned} X &= [x(0), x(1), x(2), \cdots, x(N-1)]^T \\ N &= [n(0), n(1), n(2), \cdots, n(N-1)]^T \end{aligned} \qquad (5.3)$$

Let W be NxN a wavelet transform matrix. In a vector form, the transformed output C is related to the input vector X by $C = W X$, where

$$C = \left[c(j,i),\ j = -1, 0, 1, \cdots, J;\ i = 0, 1, 2, \cdots, 2^{J-1}\right], \qquad (5.4)$$

and $J = \log_2(N)$. The indices j and i represent the scale and the position in each scale, while c(-1,0) denotes the remaining low-pass filtered coefficients.

The non-linear hard threshold is given by

$$\hat{c}(i,j) = \begin{cases} c(i,j) & ; \textit{for } |c(i,j)| \geq T \\ 0 & ; \quad \textit{otherwise} . \end{cases} \tag{5.5}$$

Hard thresholding of the transformed coefficients retains the coefficients that exceed the threshold value, while all others are set to zero.

3. Soft Thresholding

Soft thresholding is an extension of hard thresholding. It zero sets the elements whose absolute value is lower than the threshold, and shrinks the remaining coefficients by the threshold value [7].

The non-linear soft thresholding is given by

$$\hat{c}(i,j) = \begin{cases} sign(c(i,j))\left[|c(i,j)| - T\right] & ; \textit{for } |c(i,j)| \geq T \\ 0 & ; \quad \textit{otherwise} . \end{cases} \tag{5.6}$$

The advantage of this method is that the results are not as sensitive to the precise value of the threshold T, as in the "keep or kill" strategy of the hard thresholding. The disadvantage of this method is that the general shape of the signal is modified.

Thresholding method 2 and 3 are part of Donoho's method, which did not lead to improvement. Thresholding method 1, *hyperbolic thresholding*, was used exclusive in this work. Details can be found in Chapter VI and VII.

VI. TDOA ESTIMATION

Seven wavelet based denoising methods are presented and evaluated. The methods are denoising based on Donoho's method [7], denoising using the Wo-So-Ching threshold. [15], denoising using hyperbolic shrinkage [16], denoising using median filtering [14], a modified approximate maximum-likelihood delay estimation based in part on [17], denoising based on the fourth order moment, and a time varying adaptation. Figure 6.1 is a generic block diagram for all seven methods.

A. WAVELET DENOISING BASED ON DONOHO'S METHOD

Wavelet denoising, proposed by Donoho [7, 18-20], is discussed in Chapter V. This method fails at low SNR's and some results are given in Chapter VII.

B. WAVELET DENOISING USING THE WO-SO-CHING THRESHOLD

Prior to cross correlation, each one of the sensor outputs is denoised according to the Wo-So-Ching thresholding rule to increase the effective input SNR. Wavelet denoising (WD) is applied to each received signal to recover the corresponding source waveform. The restored signals are cross correlated. The TDOA estimate is given by the argument at which the cross correlation function attains its maximum value.

We define the $x(n)$, $y(n)$, $s(n)$, $n_1(n)$, *and* $n_2(n)$ sequences in vector form as

$$
\begin{aligned}
X &= [x(0),\, x(1),\, x(2),\, \cdots,\, x(N-1)]^T \\
Y &= [y(0),\, y(1),\, y(2),\, \cdots,\, y(N-1)]^T \\
S &= [s(0),\, s(1),\, s(2),\, \cdots,\, s(N-1)]^T \\
N_1 &= [n_1(0),\, n_1(1),\, n_1(2),\, \cdots,\, n_1(N-1)]^T \\
N_2 &= [n_2(0),\, n_2(1),\, n_2(2),\, \cdots,\, n_2(N-1)]^T .
\end{aligned}
\tag{6.1}
$$

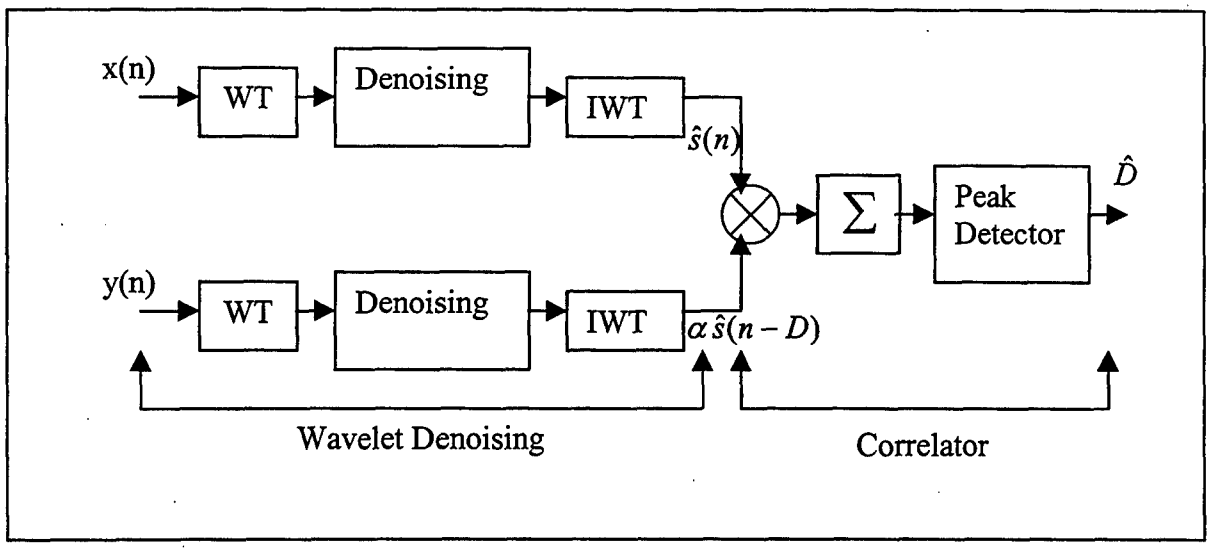

Figure 6.1: System block diagram for TDOA estimate using wavelet denoising.

The start time "0" denotes the first data point in a given block of data. The transformed output C is related to the input vector X by $C=W\ X$, . where W is a NxN orthonormal wavelet transform matrix. C can be decomposed into $C=C_S+C_{N_k}$, where

$$C_S=[c_s(j,i),\ j=-1,0,1,\cdots,J;\ i=0,1,2,\cdots,2^{J-1}] \tag{6.2}$$

$$C_{N_k}=[c_{n_k}(j,i),\ j=-1,0,1,\cdots,J;\ i=0,1,2,\cdots,2^{J-1}]\quad , \tag{6.3}$$

are the wavelet transform coefficients of the source signal vector S and the noise vector N_k (k=1, 2), respectively. The indices i and j represent the scale and the position in each scale, respectively, while $c_s(-1,0)$ and $c_{n_k}(-1,0)$ denote the low-pass filtered coefficients.

Note that, C_{N_k} is still a Gaussian vector. The main idea of the signal restoration using wavelet denoising is to adapt each $c(j,i)$ to make its value close to $c_S(j,i)$ so that a good approximation of *s(k)* can be obtained after taking the inverse wavelet transform.

The Wo-So-Ching threshold is derived according to the Neyman-Pearson criterion as it is used in hypothesis testing [15]. This criterion is stated as follows:

Let c be a Gaussian random variable with known variance σ^2. Let a test be conducted with the following hypotheses

$$H_0 : E\{c\} = \mu_0 \qquad (6.4)$$

and,

$$H_1 : E\{c\} \neq \mu_0 \qquad (6.5)$$

We will denote the acceptance of hypothesis H_0 and H_1 as D_0 and D_1, respectively. The type II error $P(D_0 / H_1)$ will be minimized for a given $P(D_1 / H_0)$ when the threshold λ is selected as follows

$$|c - \mu_0| \leq \lambda = \sqrt{2}\sigma . erf^{-1}(1-\alpha) \quad , \qquad (6.6)$$

where

c is the Gaussian random variable with variance σ^2,

μ_0 is the expectation of c under hypothesis H_0,

λ is the Wo-So-Ching threshold,

α is the type I error that is $\alpha = P(D_1 / H_0)$ and

$$erf(v) = \frac{2}{\sqrt{\pi}} \int_0^v e^{t^2} dt \quad . \qquad (6.7)$$

This denoising method discards the individual elements in C_S that are too small in magnitude. The wavelet coefficient $c(j,i)$ is regarded as totally due to noise if

$$|c(j,i)| \leq \lambda = \sqrt{2}\sigma \, erf^{-1}(1-\alpha) \quad . \qquad (6.8)$$

As a result, $c_s(j,i)$ will be modified and is given by

$$\hat{c}_s(j,i)=\begin{cases} c(j,i) & , \quad if \ \ |c(j,i)| \geq \lambda \\ 0 & , \quad otherwise \end{cases} . \tag{6.9}$$

The denoising process is applied to both *x(n)* and *y(n)*. The restored signals of *s(n)* are denoted by $\hat{s}(n)$ and $\alpha\ \hat{s}(n-D)$, respectively. The TDOA estimate is given by the location of peak of the cross correlation function of modified *x(n)* and *y(n)* coefficients.

C. WAVELET DENOISING USING HYPERBOLIC SHRINKAGE

Denoising of signals corrupted by noise uses three steps; wavelet transform, shrinkage, and inverse wavelet transform. Shrinkage reduces the value of each coefficient in magnitude by an amount related to the threshold value. The amount of the shrinkage is determined by the shrinkage method. In this section the hyperbolic method is used.

Hyperbolic shrinkage [16] is defined as:

$$\hat{c}(i,j)=\begin{cases} sign[c(i,j)]\sqrt{c(i,j)^2-\lambda^2} & ; \quad |c(i,j)|>\lambda \\ 0 & ; \quad |c(i,j)| \leq \lambda \ ; \end{cases} \tag{6.10}$$

where *c(i,j)* is the detail function of received signal, λ is the Wo-So-Ching threshold (see Equation 6.8), and $\hat{c}(i,j)$ is the modified detail function after shrinkage. The coefficients are set to the square root of the difference of the squares of the values as long as the absolute value of the coefficient is greater than the threshold. If the absolute value of the coefficient is less than the threshold then the coefficient is set to zero. Hyperbolic shrinkage can give good performance for a wide variety of signals. Other shrinkage techniques may offer better performance for specific input signals and noise conditions.

D. WAVELET DENOISING USING THE MEDIAN FILTER

In this method, a median filter (filter length 3) is applied to the first detail function of the wavelet transforms. The signals are reconstructed using the modified wavelet

coefficients.

The median filter is a non-linear one dimensional filtering technique that applies a sliding window to a sequence [14]. The median filter replaces the center point of the window with the median value of all the points contained in the window. The length of the window is very important. For example, for a stationary signal such as a sinusoid, a longer window length is better. But if the signal is a non-stationary, a short window length is better. Using the median filter may have drawbacks if one does not have a priori information about the source signal.

E. MODIFIED APPROXIMATE MAXIMUM-LIKELIHOOD DELAY ESTIMATION

An approximate maximum likelihood (AML) algorithm was proposed by Y. T. Chan, H. C. So, and P. C. Ching to estimate the TDOA of signals [17]. The general idea of this method is to attenuate the frequency bands where the noise is strong and to enhance the frequency bands where the signal is strong. To do this, we can use the pre-filters as shown in Figure 6.2. The pre-filters $H_1(f)$ and $H_2(f)$ are chosen as follows [17]

$$H_1(f)H_2^*(f)=\frac{\dfrac{G_{ss}(f)}{G_{n_1n_1}(f)G_{n_2n_2}(f)}}{1+\dfrac{G_{ss}(f)}{G_{n_1n_1}(f)}+\dfrac{G_{ss}(f)}{G_{n_2n_2}(f)}} \quad . \qquad (6.11)$$

Here $G_{ss}(f)$, $G_{n_1n_1}(f)$, and $G_{n_2n_2}(f)$ denote the auto-power spectra of s(k), $n_1(k)$ and $n_2(k)$ respectively. This choice of $H_1(f)H_2^*(f)$ is known as maximum likelihood (ML) weighting. Multiplying the denominator and nominator in Equation 6.11 by $G_{n_1n_1}(f)G_{n_2n_2}(f)$ and integrate the power spectral densities, we obtain the formula for the

weight for each subband. This tends to enhance frequency bands where the signal is strong.

The weights w_{d_i} ,used as indicated in Figure 6.3, are given by

$$w_{d_i} = \frac{\hat{\sigma}^2_{sd_i}}{\hat{\sigma}^2_{n_1 d_i}\hat{\sigma}^2_{n_2 d_i} + \hat{\sigma}^2_{sd_i}(\hat{\sigma}^2_{n_1 d_i} + \hat{\sigma}^2_{n_2 d_i})} \quad , i = 1, 2, \cdots, J \quad . \tag{6.12}$$

Since the noise density is flat and the filter gain of the wavelet transform is two, the noise power will essentially remain same after passing through each high and low pass filter. The noise power at each subband can be estimated using the formulas below

$$\hat{\sigma}^2_{n_1} = \hat{R}_{xx}(0) - \hat{\sigma}^2_s \tag{6.13}$$

$$\hat{\sigma}^2_{n_2} = \hat{R}_{yy}(0) - \hat{\sigma}^2_s \tag{6.14}$$

$$\hat{\sigma}^2_s = \arg\max \hat{R}_{xy}(\tau) \tag{6.15}$$

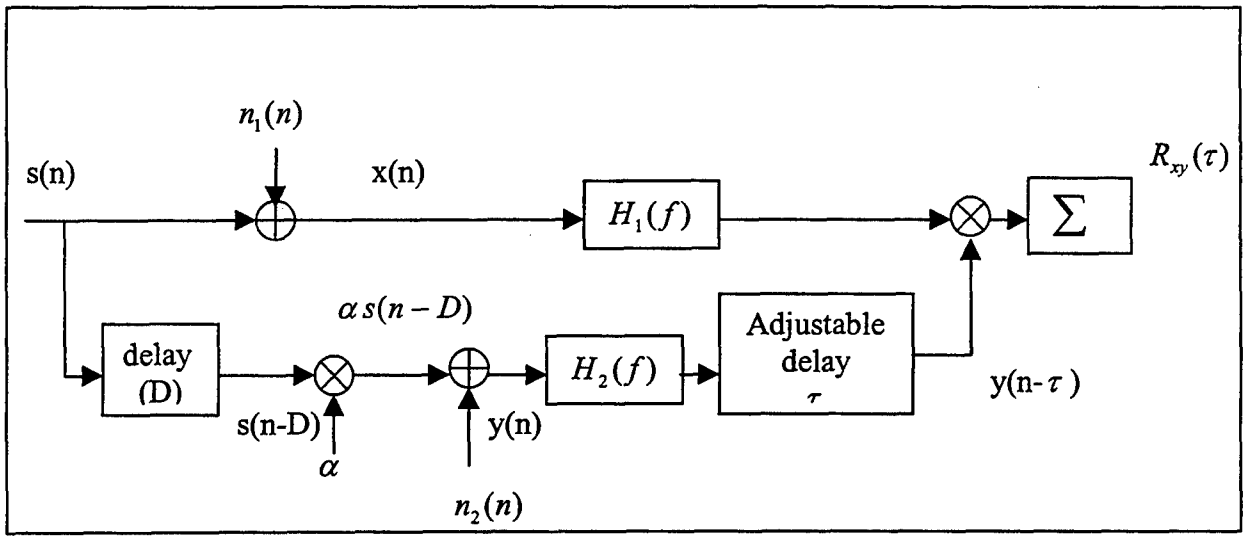

Figure 6.2: A generalized cross correlator.

$$\hat{\sigma}^2_{n_1 d_i} = \hat{\sigma}^2_{n_1} \tag{6.16}$$

$$\hat{\sigma}^2_{n_2 d_i} = \hat{\sigma}^2_{n_2} \quad . \tag{6.17}$$

The variance $\sigma^2_{n_1}$, $\sigma^2_{n_2}$ are the noise powers at each receiver, while σ^2_s is the signal power at receiver, $\sigma^2_{n_1 d_i}$, $\sigma^2_{n_2 d_i}$ represent the noise powers at the i^{th} subband after the wavelet transform. The signal power at each subband "i" can be estimated by

$$\hat{\sigma}^2_{sd_i} = \left(\frac{1}{N} \sum_{k=0}^{N-1} d_i^2(k) \right) - \hat{\sigma}^2_{n_1 d_i} \ , \ i = 1,2,\cdots,J \ ; \tag{6.18}$$

where N is the length of detail function d_i, and "i" denotes the scale.

The denoising procedure, shown in Figure 6.3, consists of the three steps. The modified subband sequences are obtained by weighting each subband by

$$d_i^c = w_{d_i} \ d_i \ ; \ i = 1,2,\cdots,J \ . \tag{6.19}$$

The modified AML method is applied to both channels. The modified subband sequences $d_1^c, d_2^c, \cdots, d_L^c$ and a_L^c are then combined to form the denoised signals.

F. WAVELET DENOISING BASED ON THE FOURTH ORDER MOMENT

1. White Noise

The correlation function for white noise is an impulse function. The samples of white noise process are uncorrelated. The correlation function of white noise process $u[n]$ has the form

$$R_u[n_1, n_0] = \sigma_0[n]\delta[n_1 - n_0] \quad . \tag{6.20}$$

A white noise stationary process has a correlation function given by

$$R_u[l] = \sigma_0^2 \delta[l] \tag{6.21}$$

and

$$S_u(e^{j\omega})=\sigma_0^2 \quad . \tag{6.22}$$

If u is a random vector of N consecutive samples from white Gaussian process, the probability density function is given by

$$f(u_0,u_1,\cdots,u_{N-1})=\frac{1}{(2\pi\sigma_0^2)^{N/2}}e^{\frac{\|u\|^2}{2\sigma_0^2}}=\prod_{n=0}^{N-1}\frac{1}{\sqrt{2\pi\sigma_0^2}}e^{\frac{(u_n)^2}{2\sigma_0^2}} \quad . \tag{6.23}$$

The samples of a Gaussian white noise process are uncorrelated and hence independent.

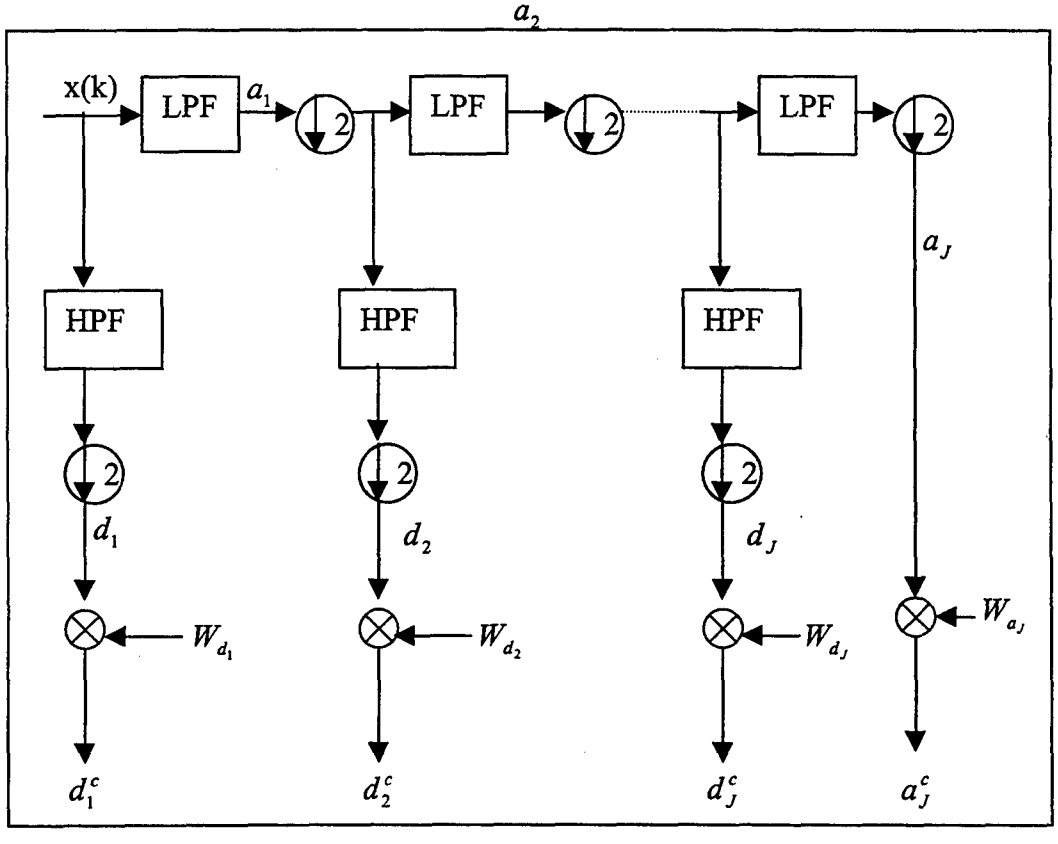

Figure 6.3: Block diagram for scaling of each subband.

2. Moments of the White Noise Process

The definitions of moments for a stationary random process are;

$$M_u^{(1)}=E\{u[n]\}=m_u \tag{6.24}$$

$$M_u^{(2)}[l_1]=E\{u[n]u[n+l_1]\}=R_u[l_1] \tag{6.25}$$

$$M_u^{(3)}[l_1,l_2]=E\{u[n]u[n+l_1]u[n+l_2]\} \tag{6.26}$$

$$M_u^{(4)}[l_1,l_2,l_3]=E\{u[n]u[n+l_1]u[n+l_2]u[n+l_3]\} \quad . \tag{6.27}$$

The first two moments are the mean and correlation function [11]. The fourth moment is given by

$$\begin{aligned} M_u^{(4)}[l_1,l_2,l_3] &= E\{u[n]u[n+l_1]u[n+l_2]u[n+l_3]\} \\ &= E\{u[n]u[n+l_1]\}E\{u[n+l_2]u[n+l_3]\} \\ &\quad + E\{u[n]u[n+l_2]\}E\{u[n+l_1]u[n+l_3]\} \\ &\quad + E\{u[n]u[n+l_3]\}E\{u[n+l_1]u[n+l_2]\} . \end{aligned} \tag{6.28}$$

If $l_1=l_2=l_3=0$

$$M_u^{(4)}[0,0,0]= \ 3\sigma_u^4 \quad . \tag{6.29}$$

3. The Wavelet Transform of White Noise

Since the wavelet transform is a linear operation, the Gaussian process remains Gaussian after passing through low and high pass filters and hence preserves the high order moments properties.

4. Fourth Order Moment of the Received Signal

The received signals are of the form

$$x(n)=s(n)+n_1(n) \tag{6.30}$$

$$y(n)=\alpha s(n-D)+n_2(n) \quad , \tag{6.31}$$

where $n_1(n)$ and $n_2(n)$ are statistically independent, zero mean Gaussian random variables. The fourth order moment estimation of the received signal is given by,

$$
\begin{aligned}
M_x^{(4)}[0,0,0] &= E\{x^4[n]\} \\
&= E\{[s[n]+n_1[n]]^4\} \\
&= E\{s^4[n]\}+4E\{s^3[n]n_1[n]\}+6E\{s^2[n]n_1^2[n]\} \\
&\quad +4E\{s[n]n^3[n]\}+E\{n_1^4[n]\} \\
&\geq E\{n_1^4[n]\} = 3\sigma_{n1}^4 \quad .
\end{aligned}
\tag{6.32}
$$

5. Mean and Standard Deviation of the Fourth Order Moment

Let $z = M_u^{(4)}$, then the mean of the z becomes

$$
E\{z\} = \frac{1}{N}\sum_{i=0}^{N-1} E\{u_i^4\} = \frac{1}{N}\sum_{i=0}^{N-1} 3\sigma_u^4 = 3\sigma_u^4 \quad . \tag{6.33}
$$

The second moment of z is given by,

$$
\begin{aligned}
E\{z^2\} &= E\left\{\frac{1}{N^2}\sum_{i=0}^{N-1}\sum_{j=0}^{N-1} u_i^4 u_j^4\right\} \\
&= \frac{1}{N^2}\sum_{i=0}^{N-1}\overline{u}_i^8 + \frac{N(N-1)}{N^2}\left(\overline{u}_i^4\overline{u}_j^4\right) \\
&= \frac{105\sigma_u^8}{N} + \frac{(N-1)9\sigma_u^8}{N} = \frac{\sigma_u^8}{N}(9N+96).
\end{aligned}
\tag{6.34}
$$

The variance of the z is given by,

$$
\begin{aligned}
\sigma_z^2 &= E\{z^2\} - E^2\{z\} \\
&= \frac{\sigma_u^8}{N}(9N+96) - 9\sigma_u^8 \\
&= \frac{96}{N}\sigma_u^8 .
\end{aligned}
\tag{6.35}
$$

If N is large, the variance of z is close to zero. We accounted for the variance in choosing a threshold, see Equation 6.42. Experimentally, this amounted to a change from $3\sigma_{n_1}^4$ to $3.1\sigma_{n_1}^4$.

6. Denoising

The fourth order moment of a detail function, which contains signal components, should be greater than $3\sigma_{nd_i}^2$, where $\sigma_{nd_i}^2$ denotes the noise power at subband d_i. Using this property the wavelet coefficients which represent noise are eliminated and the ones which represent the signal are retained.

The noise power is estimated using the formulas below

$$\sigma_s^2 = \arg\max_{\tau} R_{xy}(\tau) \qquad (6.36)$$

$$\sigma_{n_1}^2 = R_{xx}(0) - \sigma_s^2 \qquad (6.37)$$

$$\sigma_{n_2}^2 = R_{yy}(0) - \sigma_s^2 \quad . \qquad (6.38)$$

The noise power after passing through the first high pass filter is given by

$$\sigma_{n_j d_1}^2 = G.\sigma_{n_j}^2 \ /2 \quad j = 1,2 \quad , \qquad (6.39)$$

where G is the gain of the high and low pass filters. If we generalize this formula, the noise power of any detail function d_i is

$$\sigma_{n_j d_i}^2 = \frac{G^i \sigma_{n_j}^2}{2^i} \quad j = 1,2 \quad . \qquad (6.40)$$

Assuming that the filter gain is 2 then

$$\sigma_{n_j d_i}^2 = \sigma_{n_j}^2 \quad j = 1, 2 \quad . \qquad (6.41)$$

Using the fourth order moment property each detail function, see Figure 6.3, can be modified according to

$$d_i^c = \begin{cases} d_i & ; if\ E\{d_i^4\} \geq (3\sigma_{n1}^4 \pm \sigma_z^2) \\ 0 & ; otherwise \quad . \end{cases} \qquad (6.42)$$

After modifying all detail functions, the inverse wavelet transform provides the denoised signal.

F. TIME VARYING TECHNIQUE

The modified AML delay estimation method is based on the idea of attenuating the spectral components where the signal is weak. This method works well if the subband information is noise or signal only for the duration of the segment.

Since some signals are time varying or transient, the subbands can contain signal only for only part of the segment. The method is modified allowing for time variations. Each detail output is divided into two time blocks. The equations of section E are used on each segment.

VII. SIGNAL DESCRIPTION AND SIMULATION RESULTS

A. SIGNAL DESCRIPTION

Two types of test signals were used; a set of generic signals and a base band GSM signal. The signals are described in this section.

1. Generic Signals

The 13 bit Barker code sequence was used as the message to create four test signals. The signal representing one code bit is of the form $\sin(2*\pi*f*n/N)$ where $N=32$, $n=0, 1, \ldots, 31$. Signals *A, B, C,* and *D* use a value of f of *1, 4, 8,* and *12,* respectively. The generic signals are plotted in Figure 7.1.

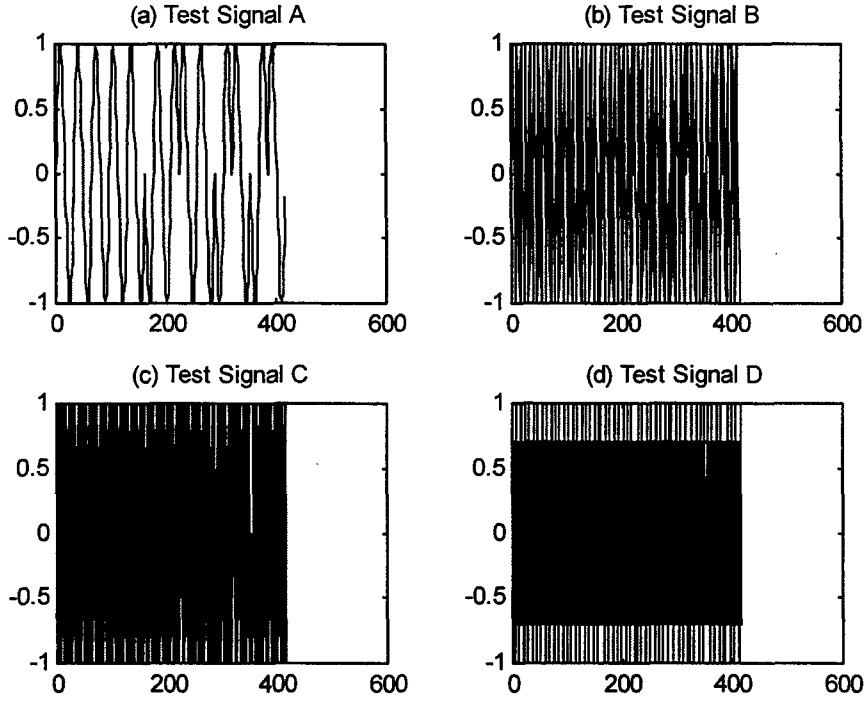

Figure 7.1: Generic signal (a) Signal A, (b) Signal B, (c) Signal C, (d) Signal D.

2. GSM Signal

According to the GSM signal properties, see Chapter II , a base band GSM signal was simulated. The I and Q channel of the GSM base band signal are shown in Figure 7.2. The MATLAB code for the GSM signal generation was adopted from [4].

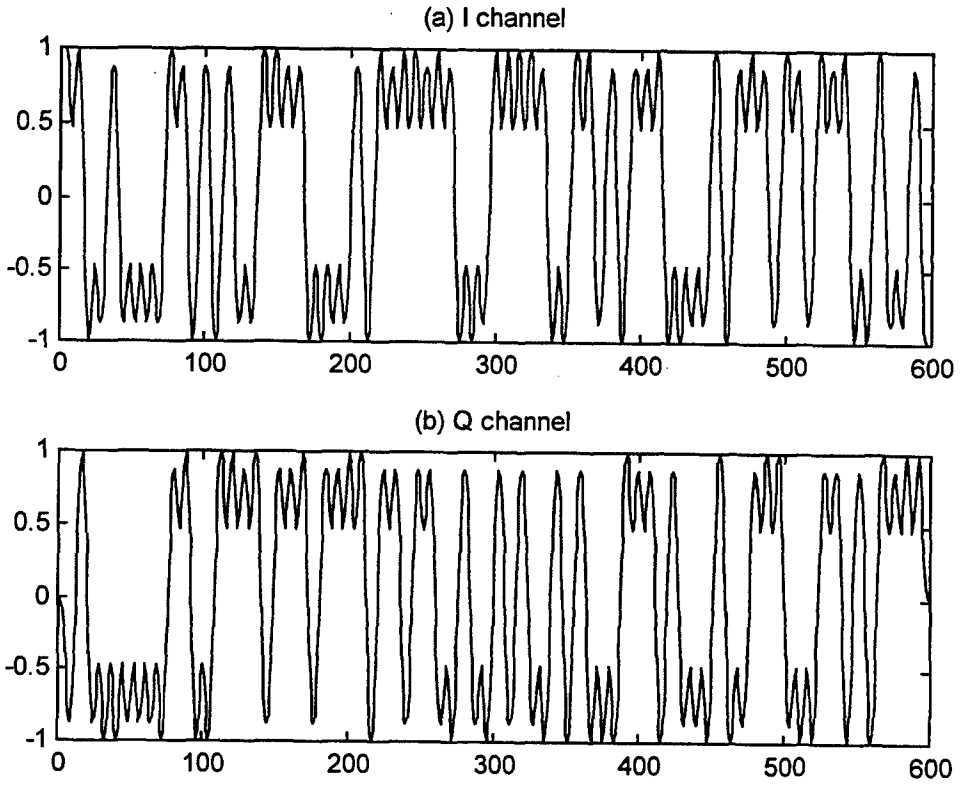

Figure 7.2: (a) I channel of GSM signal (b) Q channel of GSM signal.

B. SIMULATION RESULTS

The mean square error (MSE), as defined in Equation 4.5, is used as the criteria of goodness (i.e. low MSE denotes a small error and hence good localization). To quantify

the global improvement, we compute the sum of the MSE's (i.e., total error) for each method and compare it to the total error for the non-denoised TDOA estimate. The improvement is given in per cent. The total error is obtained by summing the MSE over the SNR's of interest (i.e., -3 to +5 dB).

1. Donoho's Method

As explained in Chapter V, Donoho proposed different types of thresholds and thresholding techniques. His methods were evaluated on the generic signals. The mean square error using wavelet denoising did not improve relative to the non-denoised version for the SNR values of interest. The mean square error obtained from the correlation of the raw signals is much smaller than when using Donoho's method. Hence Donoho's method is not investigated any further.

2. Wavelet Denoising Using the Wo-So-Ching Threshold

a. Simulation Results for Generic Signals

Figure 7.3 (a) shows that there is an slight improvement in the mean square error using Wo-So-Ching threshold method for generic signal A. As the carrier frequency is increased (Figure 7.3 (b) and Figure 7.4), the mean square error also increases. As long as the number of samples per binary bit is high there is an improvement using this denoising method, but the advantage disappears as the carrier frequency increases. The results are summarized in Table 7.1.

b. Simulation Results for the GSM Signals

Figure 7.5 shows that there is about a 28% improvement in the total mean square error using Wo-So-Ching thresholding method for the GSM signal.

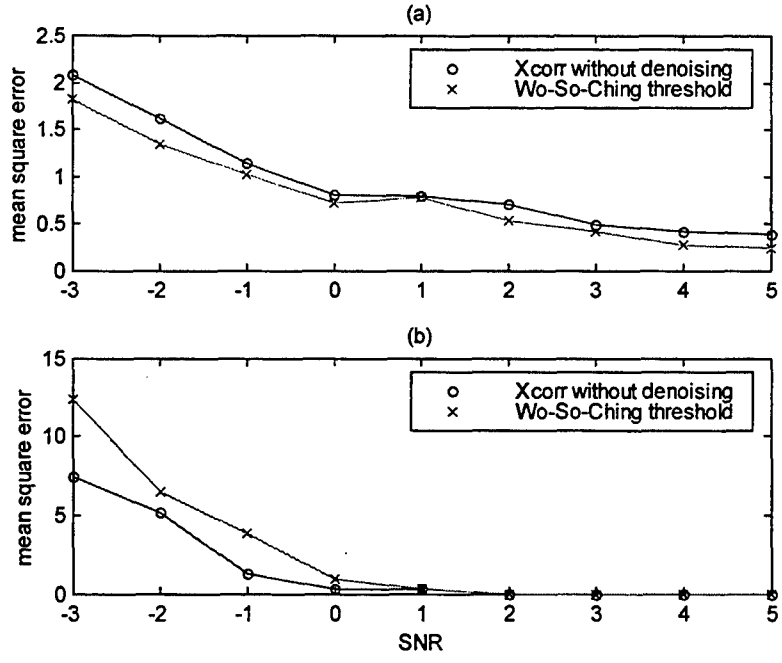

Figure 7.3: (a) MSE versus SNR with and without denoising using the Wo-So-Ching thresholding method for generic signal A. (b) MSE for generic signal B.

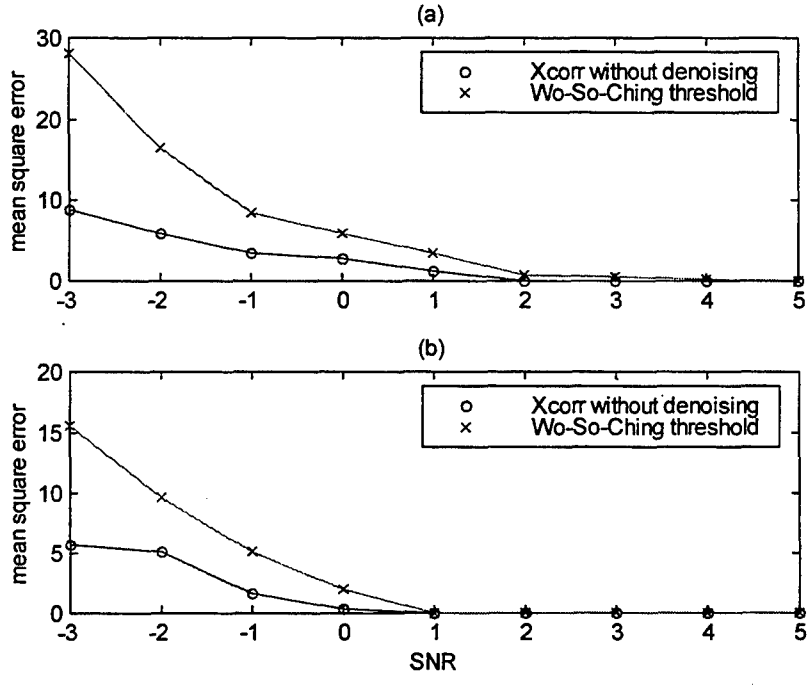

Figure 7.4: (a) MSE versus SNR with and without denoising using the Wo-So-Ching threshold method for generic signal C. (b) MSE for generic signal D.

SNR	Xcorr (A)	Wo-So-Ching threshold (A)	Xcorr (B)	Wo-So-Ching threshold (B)
5	0.385	0.25	0	0
4	0.415	0.275	0	0
3	0.485	0.425	0	0
2	0.715	0.535	0	0
1	0.795	0.78	0.32	0.32
0	0.805	0.725	0	0.96
-1	1.145	1.02	2.89	3.84
-2	1.62	1.34	4.505	6.49
-3	2.085	1.815	8.38	12.36

Table 7.1: (a) MSE versus SNR for with and without denoising using the Wo-So-Ching threshold method for generic signal A and B.

SNR	Xcorr (C)	Wo-So-Ching threshold (C)	Xcorr (D)	Wo-So-Ching threshold (D)
5	0	0	0	0
4	0	0.16	0	0
3	0	0.56	0	0
2	0.08	0.64	0	0
1	1.2	3.52	0	0
0	2.72	5.84	0.32	1.92
-1	3.52	8.56	1.6	5.12
-2	5.92	16.56	5.095	9.7
-3	8.88	28.08	5.665	15.62

Table 7.1: (b) MSE versus SNR for with and without denoising using the Wo-So-Ching threshold method for generic signal C and D.

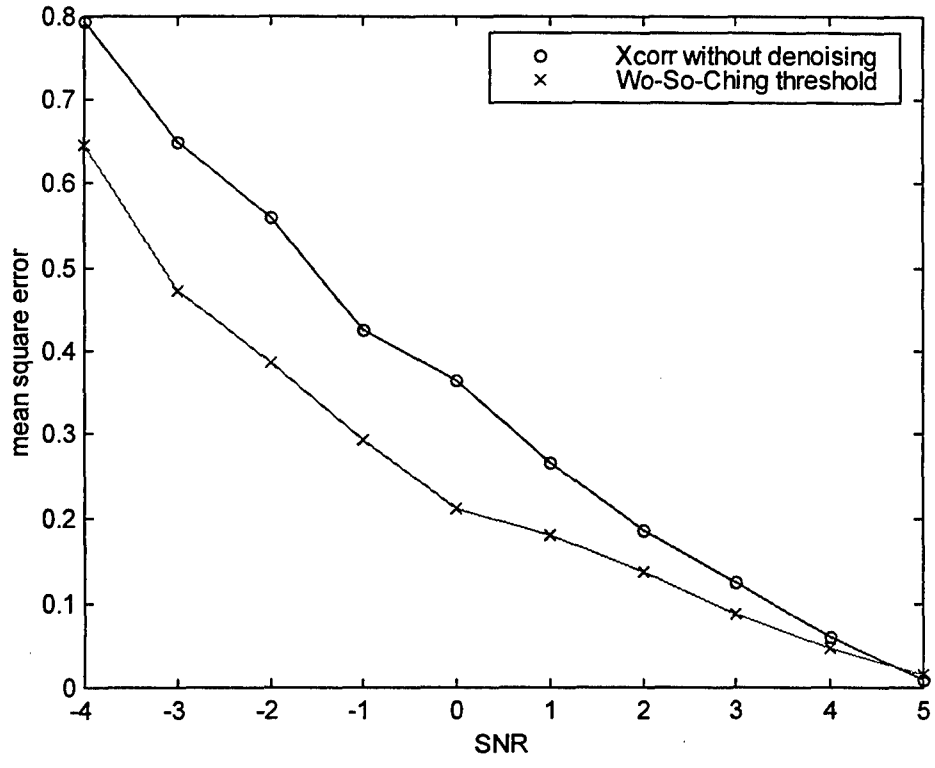

Figure 7.5: MSE versus SNR with and without denoising using the Wo-So-Ching threshold method for the GSM signal.

3. Wavelet Denoising Using Hyperbolic Shrinkage

a. Simulation Results for Generic Signals

Figure 7.6 shows that there is an improvement in the mean square error using hyperbolic shrinkage method for generic signal A and B. Again as the carrier frequency is increased (Figure 7.8), the mean square error also increases. The results are summarized in Table 7.2. Comparing Table 7.1 and Table 7.2, we can conclude that the hyperbolic shrinkage method provides better result than the Wo-So-Ching threshold method.

b. Simulation Results for the GSM Signal

Figure 7.8 shows that there is about a 48 % improvement in the total mean square error using Hyperbolic Shrinkage method for GSM signal. Comparing Figure 7.5 and 7.8 we can conclude that hyperbolic shrinkage method provides better result for the GSM signal than Wo-So-Ching thresholding method.

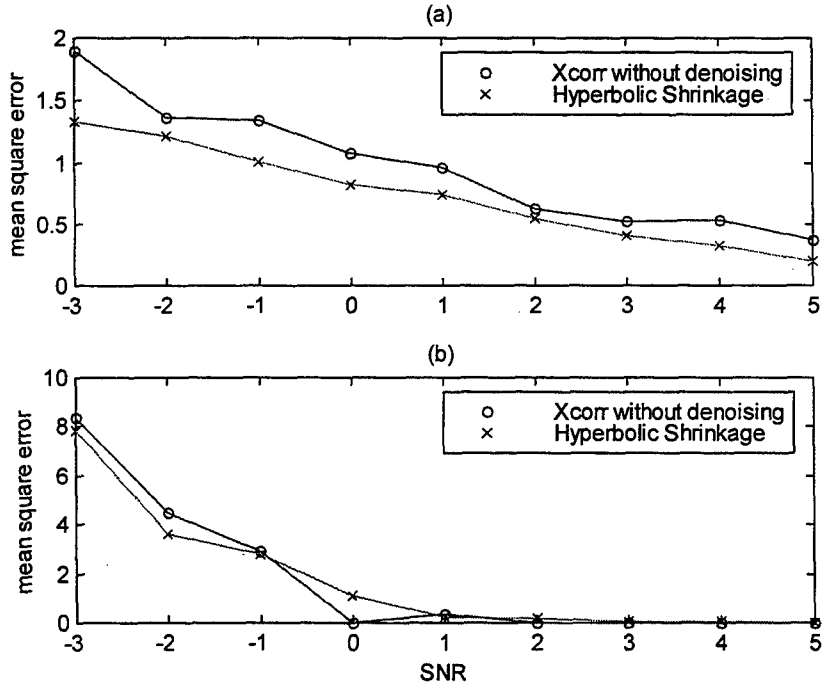

Figure 7.6: (a) MSE versus SNR with and without denoising using the Hyperbolic Shrinkage method for generic signal A. (b) MSE for generic signal B.

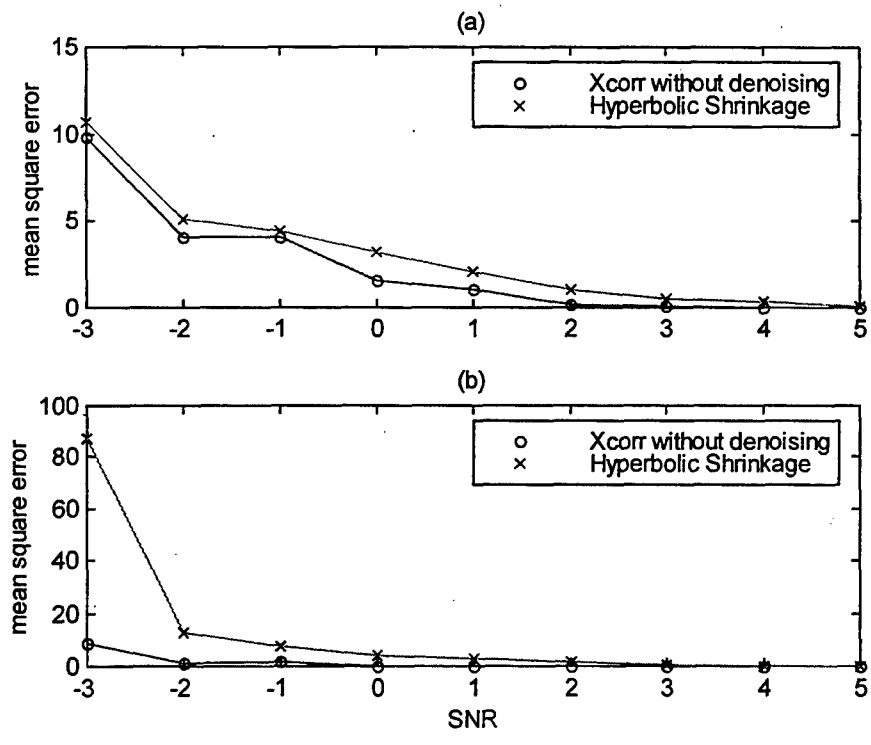

Figure 7.7: (a) MSE versus SNR with and without denoising using the Hyperbolic Shrinkage method for generic signal C. (b) MSE for generic signal D.

SNR	Xcorr (A)	Hyperbolic shrinkage (A)	Xcorr (B)	Hyperbolic shrinkage (B)
5	0.375	0.2000	0	0
4	0.53	0.3200	0	0.08
3	0.52	0.4100	0	0.08
2	0.625	0.5400	0	0.16
1	0.96	0.7350	0.32	0.24
0	1.07	0.8200	0	1.12
-1	1.345	1.0050	2.89	2.8
-2	1.36	1.2100	4.505	3.6
-3	1.895	1.3300	8.38	7.84
-4	2.425	2.2400	12.025	10.465
-5	2.57	3.5350	38.24	17.185
-6	87.41	14.5850	268.01	190.41

Table 7.2: (a) MSE versus SNR for with and without denoising using Hyperbolic shrinkage method for generic signals A and B.

SNR	Xcorr (C)	Hyperbolic shrinkage (C)	Xcorr (D)	Hyperbolic shrinkage (D)
5	0	0.1200	0	0
4	0	0.3200	0	0.24
3	0.08	0.4800	0	0.32
2	0.16	1.0000	0	1.76
1	1.04	2.0400	0	2.8
0	1.6	3.2200	0	4.015
-1	4.08	4.3800	1.645	7.625
-2	4.08	5.0800	0.96	12.735
-3	9.76	10.6450	8.76	87.35
-4	14.8	16.6750	15.385	29.055
-5	24.96	20.1500	22.97	680.8
-6	118.8	163.7250	57.635	1278.2

Table 7.2: (b) MSE versus SNR for with and without denoising using Hyperbolic shrinkage method for generic signals C and D.

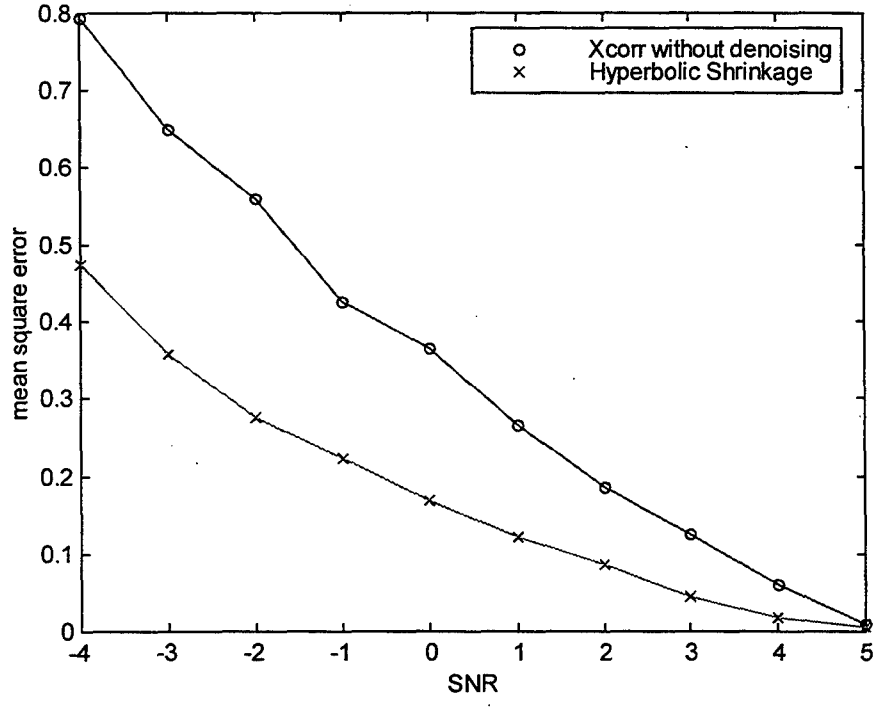

Figure 7.8: MSE versus SNR with and without denoising using the Hyperbolic Shrinkage method for the GSM signal.

4. Wavelet Denoising Using the Median Filter

a. Simulation Results for Generic Signals

Figure 7.9 shows that there is an improvement in the mean square error using median filtering on generic signals A and B. As the carrier frequency is increased (Figure 7.10), the mean square error also increases. The results are summarized in Table 7.3. Comparing Table 7.1, 7.2 and 7.3 we can conclude that median filtering has the best result for the generic signal B but for the other signals the Hyperbolic shrinkage method provides better results.

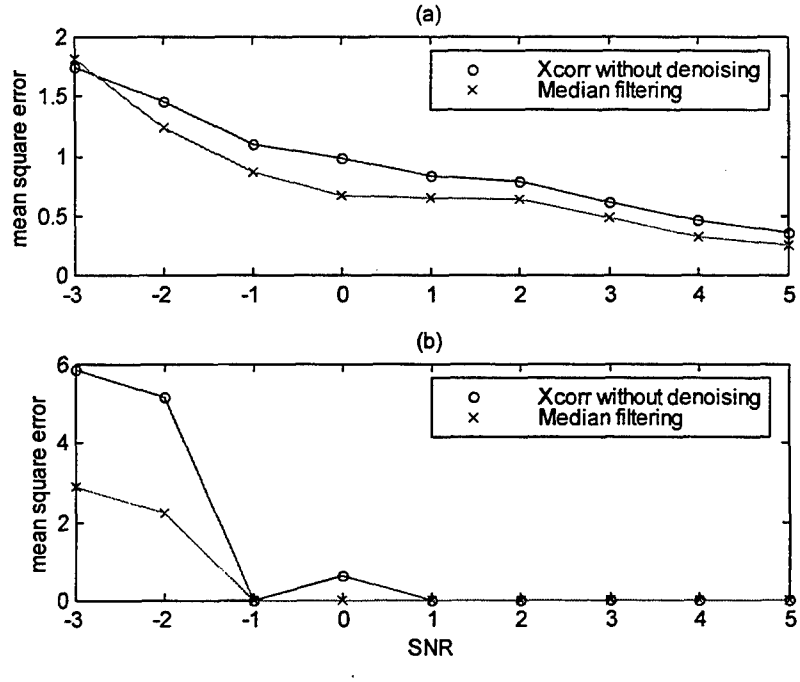

Figure 7.9: (a) MSE versus SNR with and without denoising using the median filtering method for generic signal A. (b) MSE for generic signal B.

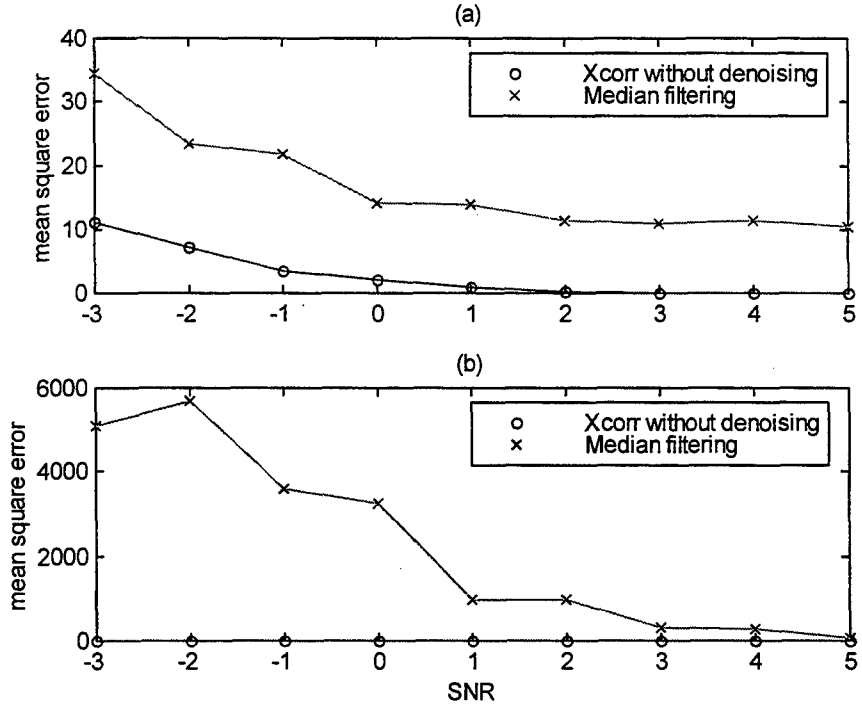

Figure 7.10: (a) MSE versus SNR with and without denoising using the median filtering method for generic signal C. (b) MSE for generic signal D.

SNR	Xcorr (A)	Median filtering (A)	Xcorr (B)	Median filtering (B)
5	0.375	0.26	0	0
4	0.53	0.325	0	0
3	0.52	0.49	0	0
2	0.625	0.635	0	0
1	0.96	0.645	0.32	0
0	1.07	0.675	0	0.005
-1	1.345	0.865	2.89	0.005
-2	1.36	1.235	4.505	2.24
-3	1.895	1.81	8.38	2.895
-4	2.425	2.125	12.025	8.855
-5	2.57	2.855	38.24	19.965
-6	87.41	28.35	268.01	200.06

Table 7.3: (a) MSE versus SNR for with and without denoising using the median filtering method for generic signals A and B.

SNR	Xcorr (C)	Median filtering (C)	Xcorr (D)	Median filtering (D)
5	0	10.52	0	67.555
4	0	11.32	0	264.57
3	0.08	10.84	0	301.49
2	0.16	11.32	0	963.45
1	1.04	13.88	0	973.63
0	1.6	14.11	0	3251.7
-1	4.08	21.825	1.645	3593.1
-2	4.08	23.425	0.96	5698.7
-3	9.76	34.415	8.76	5088.8
-4	14.8	178.33	15.385	9083.3
-5	24.96	385.47	22.97	9397.2
-6	118.8	1217.5	57.635	9916

Table 7.3: (b) MSE versus SNR for with and without denoising using the median filtering method for generic signals C and D.

b. Simulation Results for the GSM Signal

Figure 7.11 shows that there is about a 42% improvement in the total mean square error using the median filtering method for the GSM signal. Comparing Figure 7.5, 7.8 and 7.11 we can conclude that hyperbolic shrinkage method gives the best result for the GSM signal.

5. Modified Approximate Maximum-Likelihood Delay Estimation

a. Simulation Results for Generic Test Signals

Figure 7.12 and 7.13 show that there is a significant improvement in the mean square error for all generic signals when using the modified AML estimation method. The results are summarized in Table 7.4. Comparing Table 7.1, 7.2, 7.3 and 7.4 we can conclude that the modified AML estimation method gives the best result.

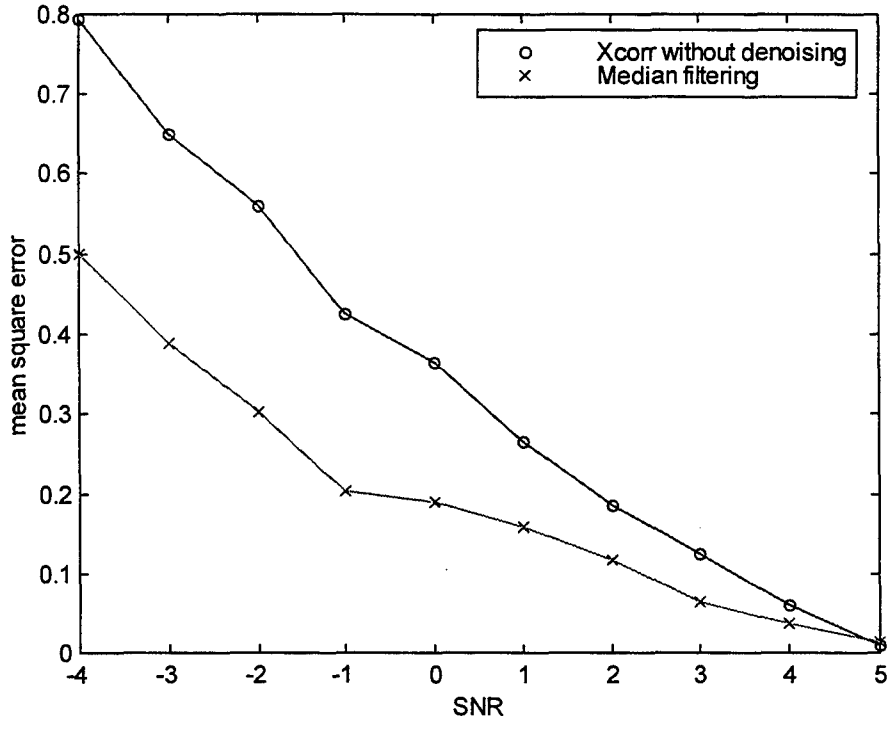

Figure 7.11: MSE versus SNR with and without denoising using the median filtering method for the GSM signal.

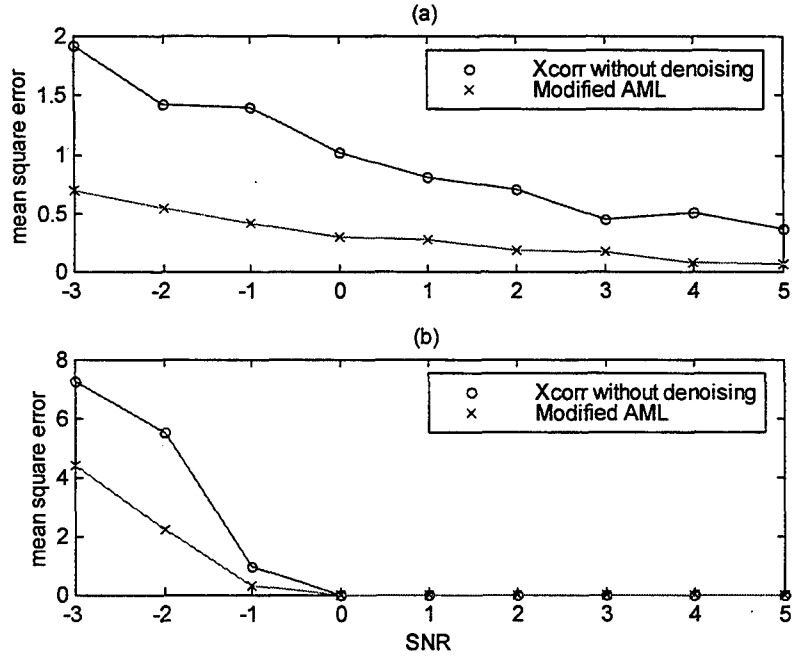

Figure 7.12: (a) MSE versus SNR with and without denoising using the modified AML estimation method for generic signal A. (b) MSE for generic signal B.

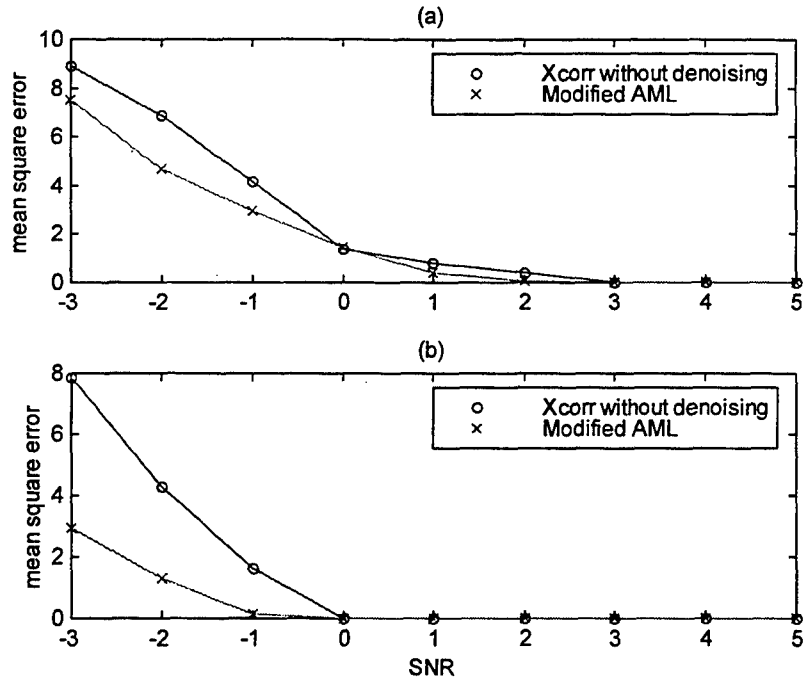

Figure 7.13: (a) MSE versus SNR with and without denoising using the modified AML estimation method for generic signal C. (b) MSE for generic signal D.

SNR	Xcorr (A)	Modified AML (A)	Xcorr (B)	Modified AML (B)
5	0.375	0.07	0	0
4	0.53	0.085	0	0
3	0.52	0.17	0	0
2	0.625	0.185	0	0
1	0.96	0.275	0.32	0
0	1.07	0.305	0	0
-1	1.345	0.42	2.89	0.325
-2	1.36	0.54	4.505	2.255
-3	1.895	0.695	8.38	4.43
-4	2.425	0.815	12.025	7.995
-5	2.57	1.26	38.24	13.085
-6	87.41	1.635	268.01	61.795

Table 7.4: (a) MSE versus SNR for with and without denoising the modified AML estimation method for generic signals A and B.

SNR	Xcorr (C)	Modified AML (C)	Xcorr (D)	Modified AML (D)
5	0	0	0	0
4	0	0	0	0
3	0.08	0	0	0
2	0.16	0.08	0	0
1	1.04	0.4	0	0
0	1.6	1.44	0	0
-1	4.08	2.96	1.645	0.125
-2	4.08	4.685	0.96	1.28
-3	9.76	7.525	8.76	2.925
-4	14.8	10.45	15.385	10.75
-5	24.96	20.395	22.97	13.35
-6	118.8	2670.8	57.635	208.15

Table 7.4: (b) MSE versus SNR for with and without denoising using the modified AML estimation method for generic signals C and D.

b. Simulation Results for the GSM Signal

Figure 7.14 shows that there is about a 79% improvement in the total mean square error using the modified AML estimation method relative to the undenoised version. Comparing Figure 7.5, 7.8, 7.11 and 7.14 we can conclude that the modified AML estimation method provides the best result for the GSM signal.

6. Wavelet Denoising Based on the Fourth Order Moment

a. Simulation Results for Generic Signals

Figure 7.15 and 7.16 show that there is a significant improvement in the mean square error using *wavelet denoising based on the fourth order moment method* for all generic signals. The results are summarized in Table 7.5. Comparing this method with the other methods, we can conclude that wavelet denoising based on the fourth order moment is the second best method.

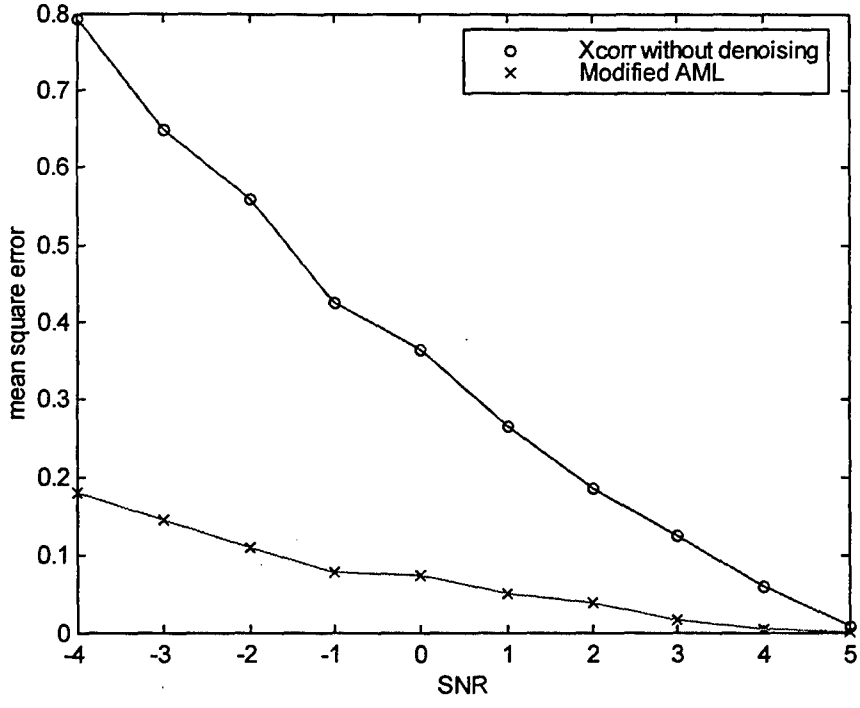

Figure 7.14: MSE versus SNR with and without denoising using the modified AML estimation method for the GSM signal.

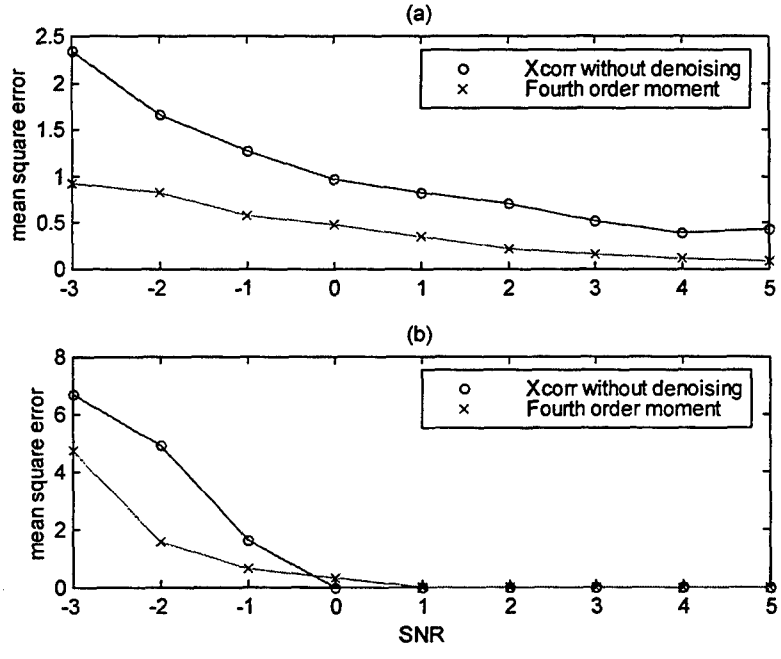

Figure 7.15: (a) MSE versus SNR with and without denoising using the *wavelet denoising based on the fourth order moment method* method for generic signal A. (b) MSE for generic signal B.

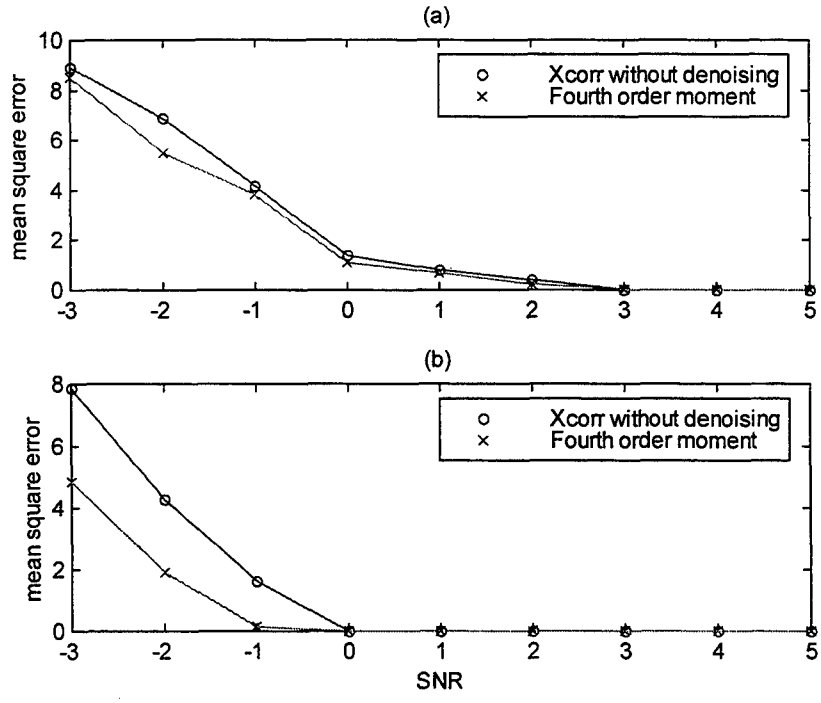

Figure 7.16: (a) MSE versus SNR with and without denoising using the *wavelet denoising based on the fourth order moment method* method for generic signal C. (b) MSE for generic signal D.

SNR	Xcorr (A)	Fourth order (A)	Xcorr (B)	Fourth order (B)
5	0.375	0.08	0	0
4	0.53	0.11	0	0
3	0.52	0.16	0	0
2	0.625	0.215	0	0
1	0.96	0.35	0.32	0
0	1.07	0.47	0	0.32
-1	1.345	0.58	2.89	0.64
-2	1.36	0.82	4.505	1.6
-3	1.895	0.92	8.38	4.73
-4	2.425	1.455	12.025	5.775
-5	2.57	1.625	38.24	10.58
-6	87.41	2.54	268.01	21.2

Table 7.5: (a) MSE versus SNR for with and without denoising *wavelet denoising based on the fourth order moment* method for generic signals A and B.

SNR	Xcorr (C)	Fourth order (C)	Xcorr (D)	Fourth order (D)
5	0	0	0	0
4	0	0	0	0
3	0.08	0	0	0
2	0.16	0.24	0	0
1	1.04	0.72	0	0
0	1.6	1.12	0	0
-1	4.08	3.84	1.645	0.125
-2	4.08	5.52	0.96	1.92
-3	9.76	8.49	8.76	4.845
-4	14.8	12.375	15.385	12.19
-5	24.96	20.86	22.97	16.595
-6	118.8	26.99	57.635	24.85

Table 7.5: (b) MSE versus SNR for with and without denoising using *wavelet denoising based on the fourth order moment* method for generic signals C and D.

b. Simulation Results for the GSM Signal

Figure 7.17 shows that there is about a 63% improvement in the mean square error using *wavelet denoising based on the fourth order moment* method. Comparing Figure 7.5, 7.8, 7.11, 7.14 and 7.17 we can conclude that *wavelet denoising based on the fourth order moment* ranks second in performance for the GSM signal.

7. Time Varying Technique

As explained in Chapter VI, we can address signals that are non-stationary (i.e., the signal does not stay in a given frequency band for the length of the segment or has modulation characteristics). In principle, in any given subband we try to find several weights. This allows us to keep the information for the frequency band when the signal is strong. Figure 7.18 allows a comparison of the modified AML method with the time varying version in which the segments are partitioned into two parts for every scale. The improvement in the total mean square error using the time varying modified AML

method is about 81%. There is no drastic improvement relative to the modified AML, but we believe that if the signal has a time varying property, the new method based on the time varying technique will give better results.

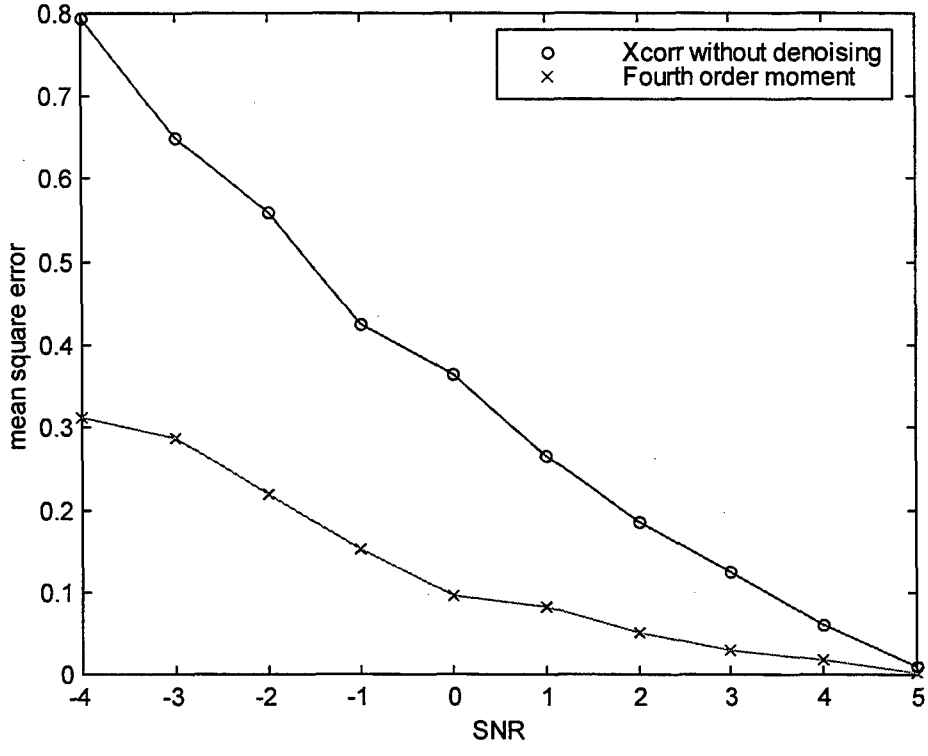

Figure 7.17: MSE versus SNR with and without denoising using the *wavelet denoising based on the fourth order moment* method for the GSM signal.

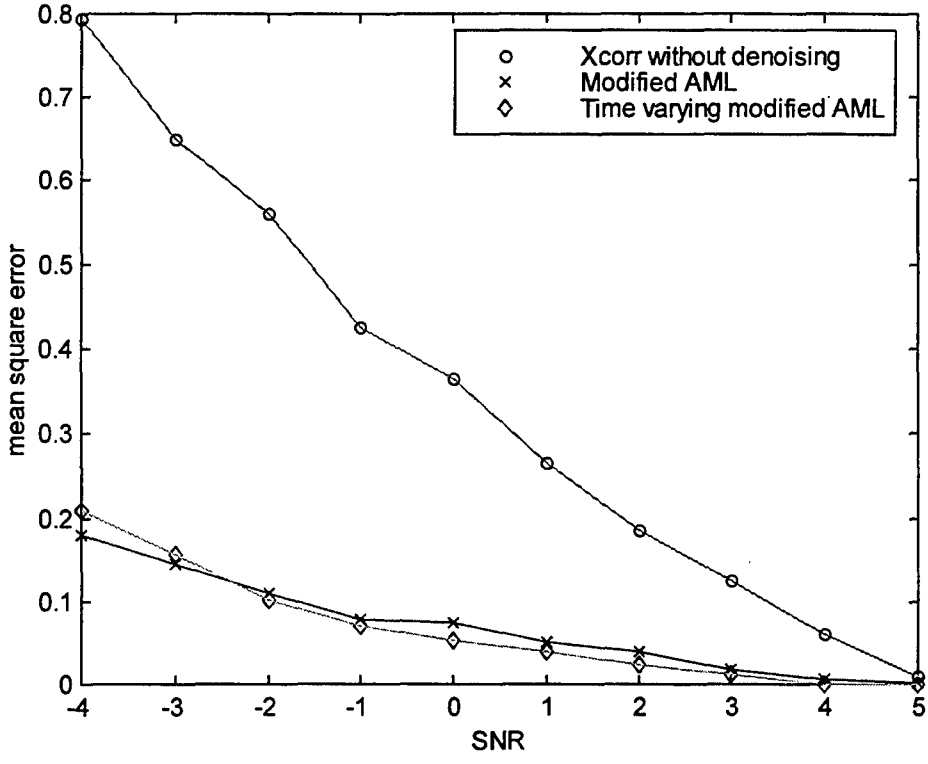

Figure 7.18: MSE versus SNR with and without denoising using the *time varying modified AML* and *modified AML technique* on the GSM signal.

VIII. CONCLUSION

A. Summary

The accuracy of algorithms to localize wireless communication units, was studied. Chapter I reviewed the need to locate cellular transmitters and some of the existing localization systems. The time difference of arrival (TDOA) method was used to locate emitters. Estimation of the TDOA was based on the cross correlation function. To increase the accuracy of the TDOA estimation, the noise in the received data was reduced (denoising). The wavelet transform was employed to minimize the noise. Several denoising methods were examined.

The MSE for all methods for the GSM signal is plotted in Figure 8.1. The *modified AML delay estimation* method provided the best result, *wavelet denoising using the fourth order moment* method ranks second. All methods provide better results than the correlation of the raw time domain signals. The time varying technique outperform the modified AML method for SNR values greater or equal to –2 dB. We believe that if the signal has time varying properties, the time varying adaptation will be the superior method.

For the GSM signal the probability of no-error is plotted in Figure 8.2 and 8.3. The Wo-So-Ching, the hyperbolic shrinkage and the median filtering techniques, see Figure 8.2, provide worse results than the direct correlation of the raw time domain signals. In these techniques, a threshold value was calculated and then according to the threshold, each coefficient was modified. These three techniques can modify the coefficients, which represent the signal in the subband. Hence we reduced the mean

square error by using these three techniques but we also decreased the probability of no-error.

The modified AML, the fourth order moment and the time varying AML techniques, see Figure 8.3, provide better results than the direct correlation of the raw time domain signals. These techniques keep the subbands or portions of it, which represent the signal. The subband, which represents noise only, is eliminated. The time varying AML method produces the highest probability of no-error.

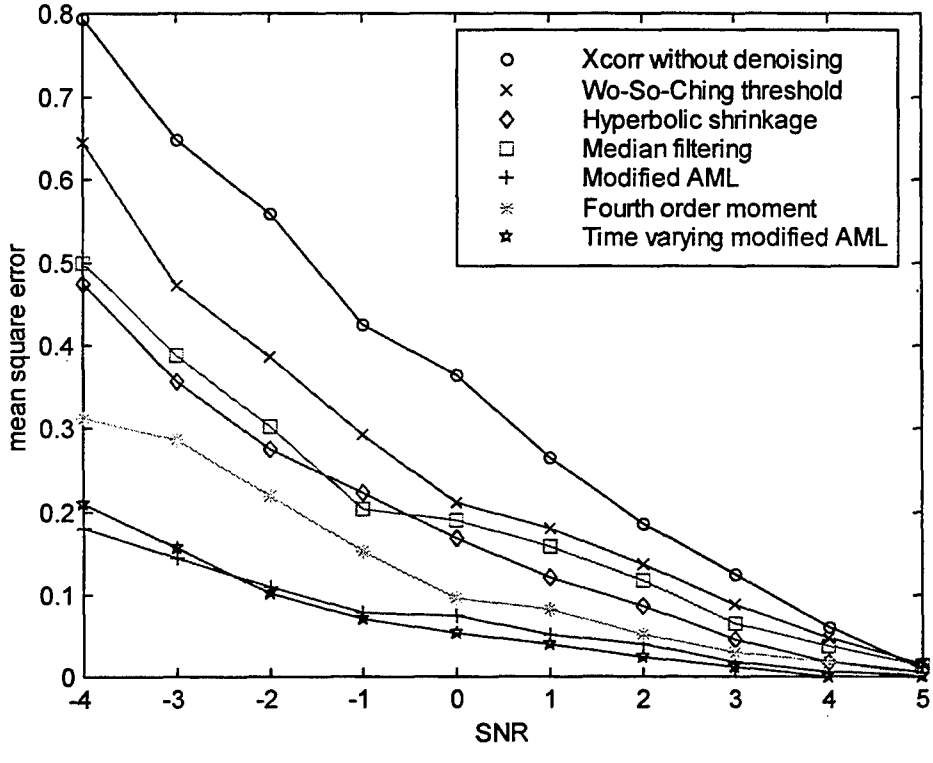

Figure 8.1: Plot of all denoising methods for the GSM signal.

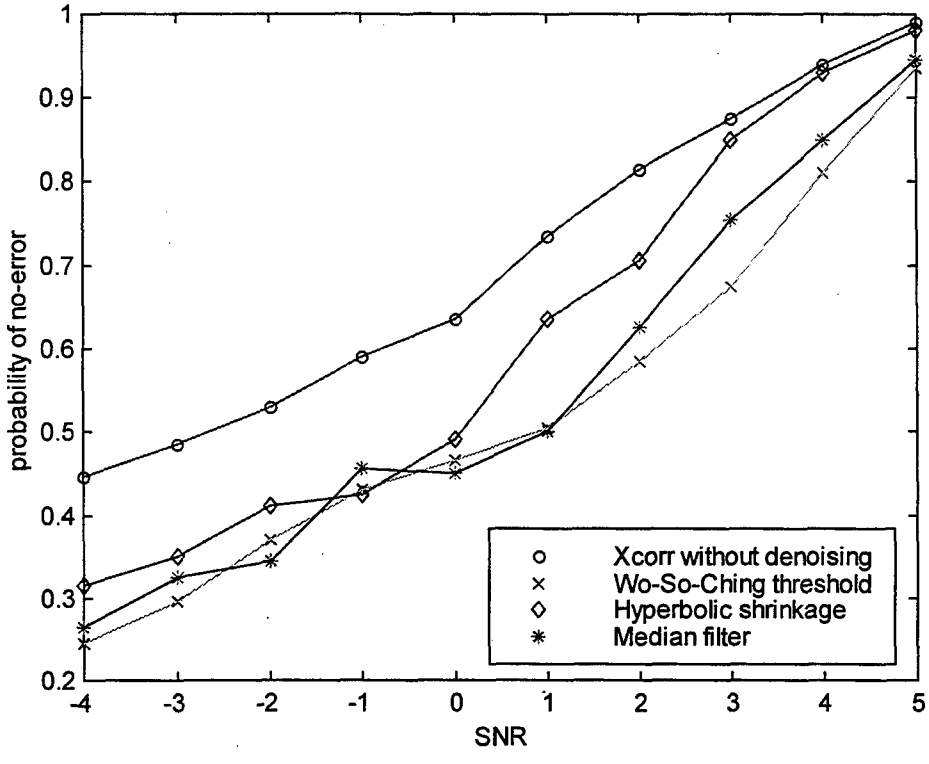

Figure 8.2: Plot of the probability of no-error for the Wo-So-Ching threshold, Hyperbolic Shrinkage and Median filtering techniques.

B. Recommendations

1. The work was done exclusively using a *base band* GSM signal. A follow on study should address GSM signals at the IF or RF level, to assess potential improvement of the MSE and hence in localization.

2. White Gaussian noise was used in the simulations. The effects of fading signals should be included in a follow on study.

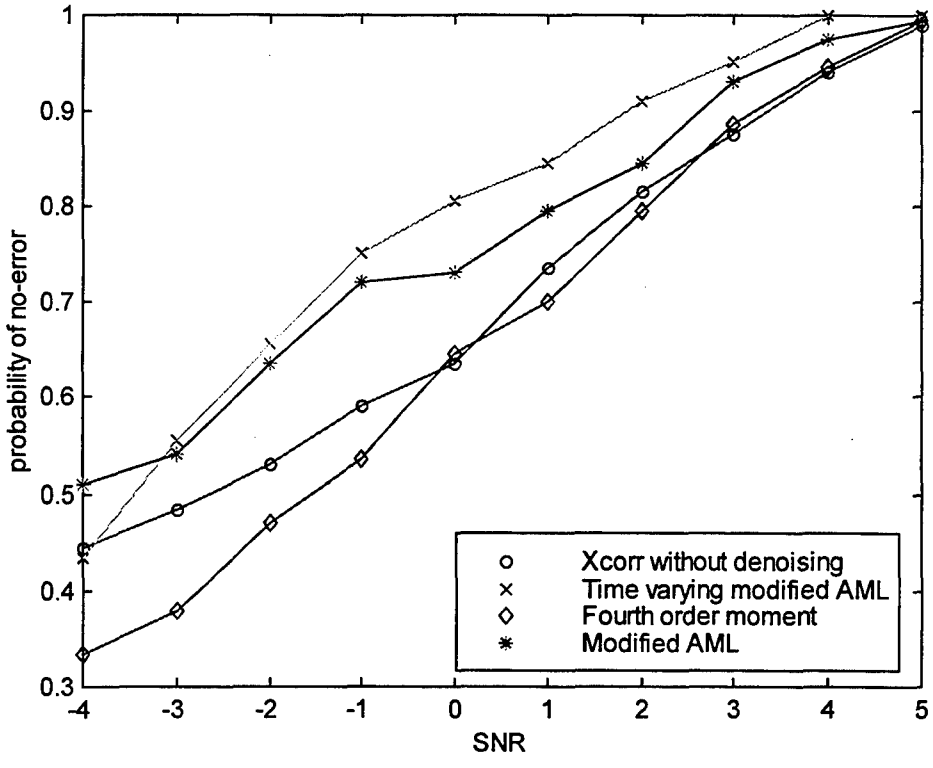

Figure 8.3: Plot of the probability of no-error for the Time varying AML, Fourth order moment and Median filtering techniques.

LIST OF REFERENCES

1. *FCC Report and Order and Further Notice of Proposed Rule Making,* FCC Docket No. 94-102, July 1996

2. Caffery, J. J. and Stuber, G. L., "Radio Location in Urban CDMA Microcells," *Sixth IEEE International Symposium on Personal, Indoor and Mobile Radio Communications*, pp 858-862, September 1995

3. Loomis, H. H., "Geolocation of Electromagnetic Emitters," October 3, 1996

4. Norre, E. A. and Jan, M. H., "GSMsim, A Matlab Implementation of a GSM Simulation Platform," December 1997

5. Rappaport, T. S., *Wireless Communications*, Prentice Hall, Upper Saddle River, NJ, 1996

6. Polikar, R., *The Wavelet Tutorial*

7. *The Matlab Wavelet Toolbox*, The Mathworks, Inc., Natick, MA, 1996

8. Haykin, S., *An Introduction to Analog and Digital Communications*, John Wiley & Sons, Inc., New York, 1989

9. Barsanti, R., *Denoising of Ocean Acoustic Signals Using Wavelet-Based Techniques*, Master's Thesis, Naval Postgraduate School, Monterey, CA, December 1996

10. Burrus, C.S., Gopinath, R.A., and Guo, H., *Introduction To Wavelets And Wavelet Transforms*, Prentice Hall, Upper Saddle River, NJ, 1998

11. Chambers, E.G., *Statistical Calculation for Beginners*, Cambridge, MA, 1958

12. Proakis, J.G., and Manolokis, D.G., *Digital Signal Processing Principles, Algorithms and Aplications*, Prentice Hall, Upper Saddle River, NJ, 1996

13. Rappaport, T. S., Reed, J. H., and Woemer, B. D., "Position Location Using Wireless Communication on Highways of the Future," *IEEE Communications Magazine*, pp 33-41, October 1996

14. *The Matlab Signal Processing* Toolbox, The Mathworks, Inc., Natick, MA, February, 1994

15. Wo, S. Q., So, H. C., and Ching, P. C., "Improvement of TDOA Measurement Using Wavelet Denoising with a Novel Thresholding Technique," *IEEE Acoustic, Speech and Signal Processing*, pp 539-542, April 1997

16. Wong, R. S. C., "Denoising of Low-SNR Signals Using Composite Wavelet Shrinkage," *IEEE Pacific Rim Conference on Communications, Computers and Signal Processing*, pp 302-305, August 1997

17. Chan, Y. T., So, H. C. and Ching, P. C., "Approximate Maximum-Likelihood Delay Estimation via Orthogonal Wavelet Transform," *IEEE International Symposium on Circuits and Systems,* pp 2501-2504, June 9-12, 1997, Hong Kong

18. Donoho, D. and Johnstone I., "Ideal Spatial Adaptation via Wavelet Shrinkage," *Biometrika*, vol. 81, pp 425-455, 1994

19. Donoho, D., "Denoising by Thresholding," *IEEE Information Theory*, vol. 41, pp 613-627, May 1995

20. Donoho, D. and Johnstone, I., "Adapting to Unknown Smoothness via Wavelet Shrinkage," *Journal of American Statistics Assoc.*, vol. 90, pp 1200-1224, December 1995

21. Stein, C., "Estimation of The Mean of a Multivariate Normal Distribution," *The Annals of Statistics*, vol. 9, pp 1135-1151, 1981

22. Harris, F. J., "On the Use of Windows for Harmonic Analysis With the Discrete Fourier Transform," *IEEE Proceedings*, Vol. 66, pp 51-83, January 1978

23. Getting, I. A., "Global Positioning Systems," *IEEE Spectrum*, pp 36-47, December 1993

INITIAL DISTRIBUTION LIST

No. Copies

1. Defense Technical Information Center.....2
   8725 John J. Kingman Rd., STE 0944
   Ft. Belvoir, VA 22060-6218

2. Dudley Knox Library.....2
   Naval Postgraduate School
   411 Dyer Rd.
   Monterey, CA 93943-5101

3. Chairman, Code EC.....1
   Department of Electrical and Computer Engineering
   Naval Postgraduate School
   Monterey, CA 93943-5121

4. Prof. Ralph D. Hippenstiel, Code EC/Hi.....3
   Department of Electrical and Computer Engineering
   Naval Postgraduate School
   Monterey, CA 93943-5121

5. Prof. Tri T. Ha, Code EC/Ha.....1
   Department of Electrical and Computer Engineering
   Naval Postgraduate School
   Monterey, CA 93943-5121

6. Prof. Alan Ross, Code SP/Ra.....1
   Department of Space Systems
   Naval Postgraduate School
   Monterey, CA 93943-5121

7. TENCAP OFFICE.....3
   Department of the Navy
   CNO/N632
   2000 Navy Pentagon
   Washington, D.C. 20350-2000